**Experimental analysis of the wear of rubber against harder materials
in reciprocating motion**

by

Yang Zhao

A thesis submitted to the Graduate Faculty of
Auburn University
in partial fulfillment of the
requirements for the Degree of
Master of Science

Auburn, Alabama
August 1st, 2015

Keywords: Rubber Wear, Reciprocating Motion, Friction, Surface Analysis, Crack

Approved by

Robert L. Jackson, Chair, Associate Professor of Mechanical Engineering
Dan Marghitu, Professor of Mechanical Engineering
David Beale, Professor of Mechanical Engineering

Abstract

This work investigated the wear performance of rubber when contacted against harder composite materials through experimental analysis. The focus of this thesis was to find the optimal type of rubber and the composite material.

Different kinds of rubber including SBR/NR mix, 60 duro, SBR/NR mix, 80 duro, Butyl, 50 duro and 100% NR, 65 duro are used. Various composite materials such as Polyvinyl chloride (PVC) and fiber-reinforced plastic (FRP) were also used. The experiments were performed using a pin on disk set up of UMT-3 at the loads and speeds that are in the boundary lubrication regime under air, water and slurry. Preliminary tests will be conducted to find a combination of load and speed that results in a measurable amount of wear in a reasonable amount of time. Surface metrology were performed using a precision stylus profilometer. Wear of rubber was measured based on the wear volume, average wear depth without cracks and max wear depth with or without cracks. In order to thoroughly characterize the mechanism of the rubber wear, an indention test without sliding was conducted to compare with the sliding tests. In addition, wear of the opposite composite materials were analyzed according to the weight lost and surface roughness change before and after each slurry test.

Based on the results, it showed that the Butyl, 50 duro rubber had the best anti-wear performance. And the optimal contact pair can be put forward for evaluating possible design improvements, including the use of alternative materials.

Acknowledgments

I would like to acknowledge everyone who helped and supported me through my master studies over the past two years. First and foremost, I want to express my gratitude and gratefulness to my caring parents and sister for their selfless support and encouragement.

I wish to acknowledge my advisor, Dr. Robert Jackson for his great motivation, support and guidance during my study. Much thanks to Dr. Hamed Ghaednia for designing the test rigs and Tim Hall and Matthew Sprinkle for helping with the tests. I also want to express my thanks to my lab mates, Xianzhang Wang, Sara Pope, Hamid Ghaednia, Yang Xu, Xiaohan Zhang and Swarna Saha. I would like to thank my committee members, Dr. Dan Marghitu and Dr. David Beale, for their support and guidance. I should also acknowledge all my friends in Auburn for their friendship.

Table of Contents

List of Tables

List of Figures

List of Abbreviations

HUMWPE   Ultra-high-molecular-weight polyethylene

UMT   Universal material tester

NR   Natural Rubber

SBR   Styrene-butadiene rubber

FRP   Fiber-reinforced plastic

PVC   Polyvinyl chloride

COF   Coefficient of Friction

D   Crack size

l Crack mean free path

D_1 Short-distance cut-off length

V   Volume of rubber wear

v Average velocity of the crack tips

N_0 Cracks on the nominal contact area

ζ   Number of order unity

A_0 Nominal contact area

L   Sliding distance

v_0 Sliding velocity

P	Ratio between the rubber contact area and the nominal contact area
λ	Surface wavelength
ω	Pulsating deformation frequency
α	Heat transfer coefficient
A_1	Real contact area
A_m	Nominal macro-asperity contact area
α_1	Heat transfer coefficient for stationary contact
α_{spread}	Spreading heat resistance
p	Nominal contact pressure
h_{rms}	Component root mean square roughness
k_0	Heat conductivity of the rubber
LVDT	Linear Variable Differential Transformer

Chapter 1

Introduction and literature review

1.1 Brief description of polymer wear

The behavior of wear is generally affected by the material types, environmental and operating conditions and geometry of the wearing bodies. Generally, the chemical stability, mechanical properties of materials and operating conditions are the fundamental factors when we consider about the mechanisms of particular wear type. [1]

The wear mechanics of non-metallic solids has significant differences compared with the wear of metal materials. Analysis of the difference is meaningful to find new materials which have better tribological performances to meet the requirements cannot be satisfied by the traditional metallic materials. It is mentioned that "when a polymer slides against another polymer, the cohesively weaker polymer is worn preferentially to form a transfer film on the cohesively stronger polymer." [2]

The general factors affecting the wear of polymer are the hardness, roughness and the surface energy of the countersurface. In the practical engineering applications, the material of the countersurface should be much harder and smoother than the polymer itself [3]. In this way, it will not abrade the opposite polymer surface excessively. And for the surface roughness, generally, the roughness should be as low as possible to reduce the possibility of the polymer abrasion because when the surfaces get rougher, the wear rate is accelerated. This can be explained by figure 1. But there is an exception, the sharp asperities of the optimally smooth surface may have a positive effect on controlling abrasion. The polymer debris can act as a 'transfer film' to cease to abrade. That is why the wear rate for the excessively smooth counterface may be higher than the optimally

smooth counterface. [4] Also when sliding at high speeds, roughness dependence seems to be insensitive to the wear rate, which is probably because the dominant wear mechanism changed. Besides the surface roughness, the other factor affecting the wear rate of polymer is asperity height distribution of the countersurface [5]. It is recorded that some significant differences were found in the wear rate between surfaces with a Gaussian asperity height distribution and surfaces with a non- Gaussian distribution. In addition, the surface energy of the countersurface may influence the wear rates of a polymer by affecting the wear debris shapes and the formation of transfer film [6].
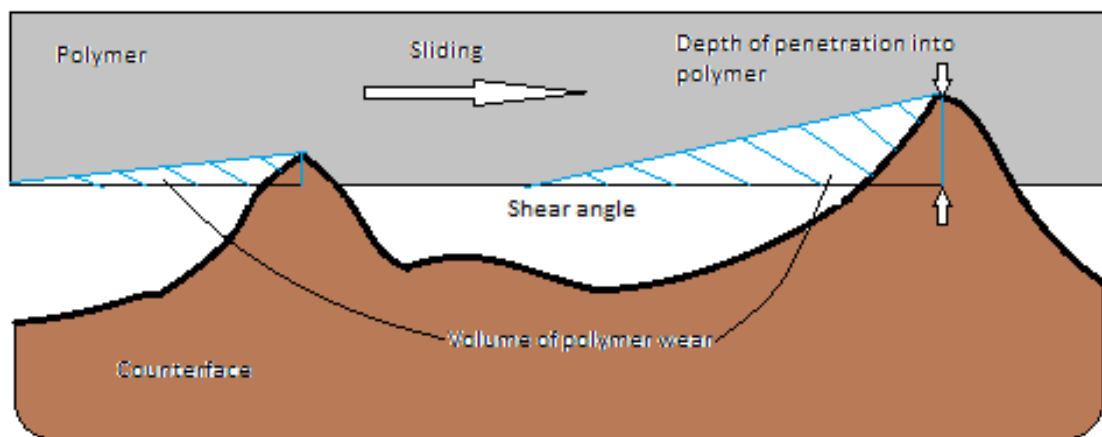
Figure 1. Volume of polymer removal against harder rough surface [7]

Because of the relatively low melting temperature and the low thermal conductivity of most polymers, melting wear can occur on the contact region. When a polymer sliding on a counterface, which usually has a higher melting point, the frictional heat in confined to a thin surface layer and the molten or soften polymer forms a thin low-shear-strength interfacial layer between the counterface and the polymer. [7] Due to the loss of the molten polymer, the wear rate will be severe. But, however, the continuous

surface melting wear may not occur if the countersurface has a very high thermal conductivity. In this case, the contact temperature may not reach the 'critical temperature' which initiates the severe wear of the polymer. Generally, a severe abrasion of the relatively soft polymer surface can occur without the continuous melting wear because of the combined effect of high elevated contact temperature and the rough countersurface.

In addition, if the motion of the polymer against the hard counterface is reciprocating sliding contact causing many stress cycles, it may lead to a fatigue wear of the soft polymer. An experimental example [8] is that due to the ignition of fatigue wear, the wear rate of ultra-high-molecular-weight polyethylene (HUMWPE) is increased after a long sliding duration when it slid against a smooth steel surface. During the first 500 km sliding, it is in the early stage of wear. The mechanism of this initial slow wear are mainly adhesion and deformation with the initiation of cracks in the polymer. While after a long sliding duration, under the fluctuating stresses of the cyclic contact, more cracks are developed. With the growth and convergence of the cracks, wear debris releases into the contact interface and increases the wear rate. In this long-term rapid wear stage, fatigue wear becomes the dominant mechanism instead of the previous adhesive wear or transfer film. In addition, contact stress plays a very important role in the mechanism transition. Under the conditions of heave loads, smooth counterfaces and long sliding distances, the possibility of fatigue wear increases.

Generally, the additions of lubricants will decrease the coefficient of friction and reduce the wear of polymer. For the fundamental lubricant like water, it may form a transfer film on the contact region which can provide sufficient lubrication. [7] For rubber wear, adding water may have the hydrodynamic lubricating effect on decreasing

the wear rate. Due to hydrodynamic lift, with the lubrication of water in the contact

region, when the velocity is increased, the wear rate will decrease.

1.2 Wear in the rubbery state

Due to its unique characteristics of low wear and high friction coefficients (COF),

rubber and rubber like polymer materials are applied to pipe-lining and tires [7]. Rubber

is a natural polymer and has the same wear mechanisms such as abrasion, adhesion,

fatigue, corrosion and the thermal decomposition described above [9]. In its rubbery

state, the long linear molecular structure of rubber can form an amorphous solid by

'coiling and tangling together' [7] to sustain an extremely large strain. In addition, rubber

molecules will arrange themselves in the direction of the applied strain. In this way,

relatively high strain can be maintained with a low tensile modulus [7] [9]. The material

properties described above make the contact mechanics of rubbers unique compared with

other materials. Several wear mechanisms are introduced below which are particularly

adaptable to rubbery state materials.

Schallamach Waves

When rubber contacts against a harder material with a sliding movement, its low

tensile modulus will result in a larger true area of contact and a tangential movement

which direction is parallel to the sliding without fracturing or releasing wear debris. [7]

The latter can be explained by the sliding mechanism of the Schallamach wave [10],

which is the minute ripples in the rubber surface during the rubber sliding process. By

van der Waals force, the real contact area of rubber strongly adheres to the most

counterfaces and cannot move without very large tangential force. But under smaller

tangential force, small parts of the contacting rubber comes apart from the contact region and forms a ripple between the rubber and the counterface inside the rubber body. With the movement of the ripples in the tangential direction, the rubber body will have a slight tangential movement forward. At lower sliding speed, the wave generally moves faster than the two contact parts. However, this mechanism may fail when the speeds of the wave and the sliding are same. The melting wear of the rubber caused by the frictional heating may occur.
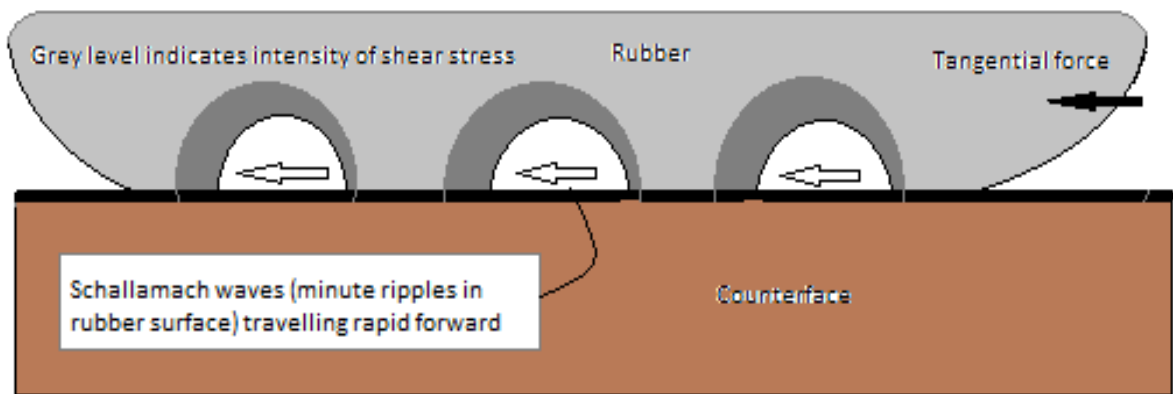
Figure 2. Schallamach wave mechanism of sliding between rubber and a hard counterface [7]

Roll formation

For a material like rubber, forming wear debris requires a lot of frictional work because rubber has the ability to sustain large strains to avoid fracture. The tangential forward movement by adhesion of rubber make the rubber roll itself, and become the 'roll formation' wear. [9]
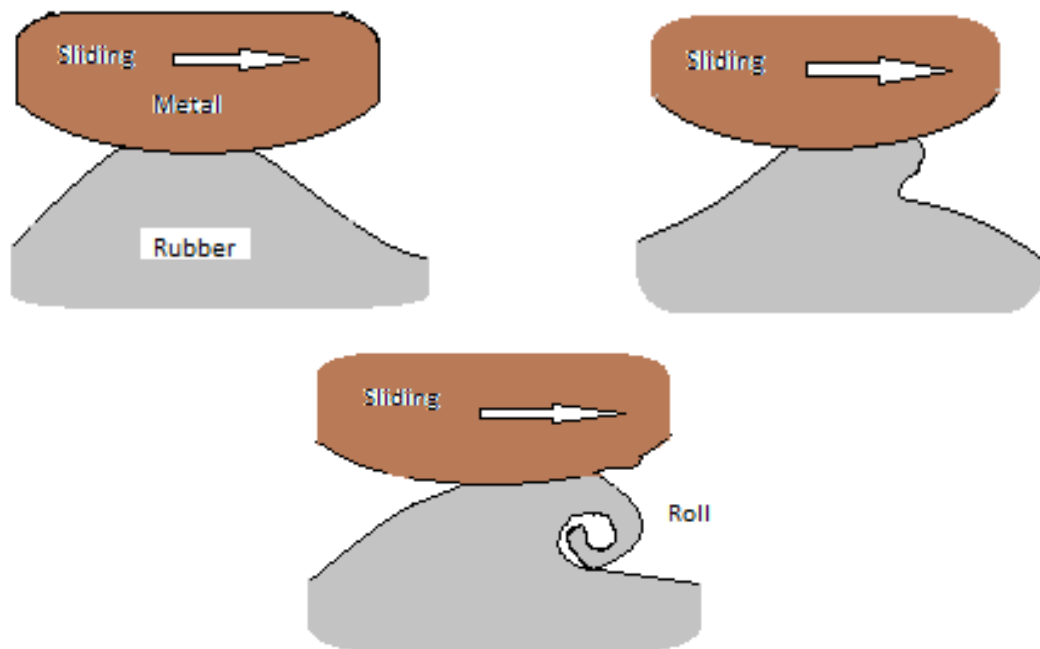
Figure 3. Mechanism of 'roll formation' on rubber surface [7]

1.3 Literature review of rubber wear

Qualitative theory of rubber friction and wear

Persson et al. [11] put forward a qualitative theory of the relation between the friction force and surface roughness as well as surface wear of the sliding rubber when contacted with a hard substrate. Because rubber has a "very low elastic modulus" and the high internal friction over a wide frequency region, it has very peculiar friction and wear properties. They may be related to the elastic instabilities during sliding, like the Schallamach wave, or the energy dissipation via internal damping. The amount of rubber worn is related to the response state of rubber, which is determined by the temperature, sliding velocity and the shear stress frequency. For example, at room temperature under a low frequency shear stress, little wear will be caused. In this case, the rubber is in the elastic state. While at low temperature and very high frequencies, the amount of wear may be very significant because in this case, the state of rubber is glassy. A very important reason for the larger amount of rubber wear at low temperature is the crack propagation. [12] The reason for the propagation is the thermal excitation over the energy barriers, which causes the rubber molecule to break instead of elastically deform. In addition, sliding velocity plays an important role in rubber wear. Generally, at large velocities, the rubber may be in the glassy state, which is more likely to result in large wear. Likewise, rubber will have enough time to deform elastically and to fill the void between the rough contact surfaces at slowly sliding velocities. In addition, at low frequencies the rubber will be below the glassy region. In this way, the wear of the rubber will be smaller.

Theory of powdery rubber wear

Persson [13] also described a theory of mild rubber wear in a subsequent work which included the wear particle sizes distribution and the calculated wear rate. Generally, the detached small rubber particles are formed when rubber is sliding on a harder rough surface. Two basic steps can clarify this wear process, the formation of the rubber defects and the propagation of the cracks. It is also noted that the coefficient of friction (COF) has an important influence on the wear rate of rubber sliding against harder rough surfaces. The first one is the crack propagation caused by the strong tensile stress which is initiated by the friction force. The second is the temperature increase caused by the frictional energy dissipation, which may cause stress concentration, bond-breaking and even thermal decomposion.

The wear particle sizes distribution and wear rate was theoretically considered. For rubber sliding against a harder surface for a sliding distance of *L*. The theoretical results appear to be in good agreement with the experimental data. The theoretical method from Persson [13] is explained here.

Wear particle distribution

The crack size, which is the same to the rubber particle size, is *D*. *l* is referred as the crack mean free path and D_1 is introduced as the short-distance cut-off length.

$$\emptyset(D) = l^{-1}e^{-(D-D1)/l},\qquad(1)$$

The cumulative probability

$$\int_{D_1}^{D}\emptyset(D')\,dD' = 1 - e^{-(D-D_1)/l},\qquad(2)$$
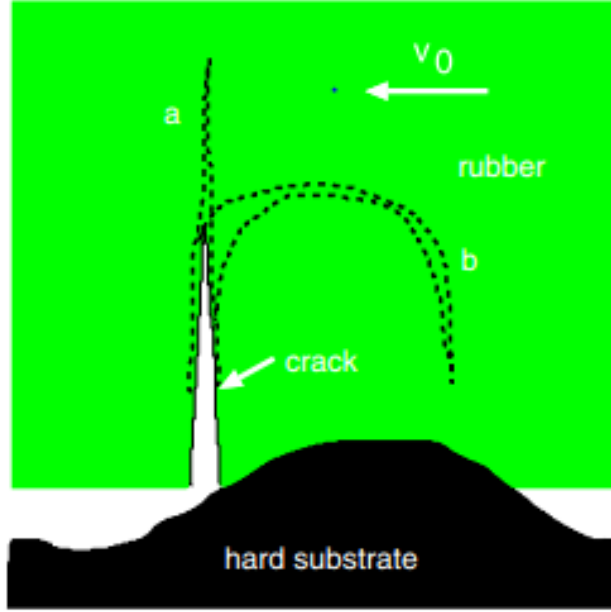
Figure 4. A Crack can propagate normal to the surface a or 'turn around' b and produce a wear particle. The crack is on the average strait over a distance l. [13]

Wear rate

$$\frac{dV}{dt} = N_0 \int \frac{\pi D^3}{6} \frac{v(D)}{l} \Psi(D) dD, \tag{3}$$

Where V is the volume of rubber wear. In addition, the $v(D)$ represents "the average velocity of the crack tips when the crack has the size D". And N_0 refers to the cracks on the nominal contact area,

$$N_0 = \frac{\zeta A_0}{D_1^2}, \tag{4}$$

where ζ is a number on the order of unity, and A_0 is the nominal contact area.

$$\frac{dV}{dt} = C A_0 v_0, \tag{5}$$

The sliding distance $L = v_0 t$, v_0 is the sliding velocity.

The wear rate

$$\frac{dV}{dL} = CA_0,$$ (6)

where

$$C = \frac{\pi\zeta\, D_1}{6l} \frac{\int_{D_1}^{\infty} dD (D/\,D_1)^3 e^{-D/l}}{\int_{D_1}^{\infty} dD [\frac{v_0}{P(\zeta)v(D)}] e^{-D/l}},$$ (7)

and $P(\zeta) = A(\zeta)/A_0$, is the ratio between the rubber contact area at the value of ζ and the nominal contact area. The magnification ζ can be related to the rubber particle size as $D \approx \frac{1}{q} = \frac{1}{q_0\zeta}$, where q_0 is the reference wavevector and q is the wavevector of surface wavelength roughness.

Role of frictional heating in rubber friction

In another work, the effect of the high temperature in the contact region which is caused by the energy dissipation on the rubber friction was analyzed and an equation for frictional heating was derived by Persson [14]. Generally, when a rubber block is sliding with the velocity of v on a rigid material surface with multi-scale roughness with the wavelength of λ, the pulsating deformation frequency will be $\omega \approx v/\lambda$. The real contact area will affect the energy dissipation and the temperature field, as well as the flash temperature and the background temperature. A hot tracks effect which labels the kinetic thermal interaction was also used to explain the influence of temperature on rubber

friction. In addition, a heat transfer coefficient was applied to describe the heat energy transfer at the sliding interface.

The heat transfer coefficient α between rough surfaces is [15] [16],

$$\alpha \approx \frac{A_m}{A_1 \alpha_1} + \frac{1}{\alpha_{spread}}, \tag{8}$$

where A_1 refers to the real contact area and the A_m is the nominal macroasperity contact area and α_1 is the heat transfer coefficient for stationary contact due to "scattering of phonons at the contact interface" which is changed slightly and the α_{spread} is the spreading resistance due to "the diffusive thermal interaction between the heat flow in rough surface contact", which is affected by the sliding motion and velocity dependent.

$$\alpha_{spread} \approx \frac{2}{E^*} \frac{p}{u_0} \left(\frac{f_0(v)}{k_0} + \frac{f_1(v)}{k_1} \right)^{-1}, \tag{9}$$

Where p is the nominal contact pressure and $u_0 \approx 0.5 h_{rms}$, the length parameter with h_{rms} the component root mean square roughness when the wavelength less than the scale of the contact area, k_0 and k_1 the heat conductivity of the rubber and the hard rigid material. In addition, with the definition of [14]

$$f_0(v) = 1 \ \ for \ \ v < D/R$$

$$f_0(v) = \frac{D}{vR} \ \ for \ \ v > D/R$$

$$f_1(v) = 1 \ \ for \ \ v < D'L/R^2$$

$$f_1(v) = \left(\frac{D'L}{vR^2} \right)^{1/2} \ \ for \ \ v > D'L/R^2$$

Criteria for crack initiation during rubber abrasion

Fukahori et al. [17] analyzed the crack initiation of the rubber abrasion process experimentally using a rubber-blade test and theoretically by a FEA simulation. They postulated that in the slip stage of stick-slip motion, the micro-vibration [18] was generated and it is the origin of the initial crack. The crack growth angle was also considered. At the location of the maximum tensile stress, a crack growth angle of 30° ~ 50° results. With the continuous application of the normal load, the initial crack will propagate with the reduction of the crack growth angle until the abrasion reaches a steady state. While for the upper surfaces with the sharp edges, they thought the reason for the crack initiation was the stress concentration and that the cracks should be distributed randomly.
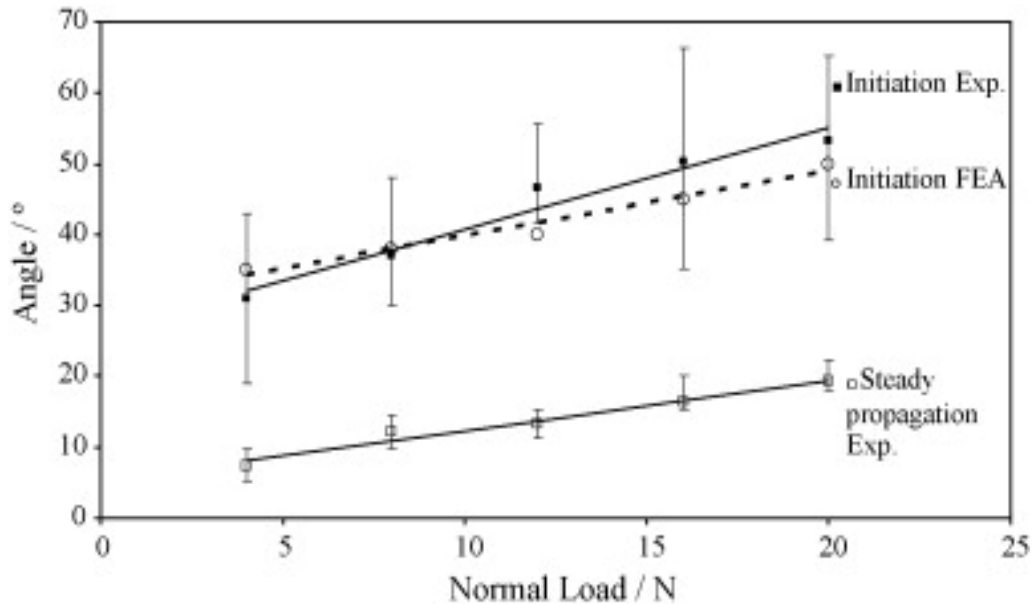
Figure 5. Crack growth angle against normal load during crack initiation from both the experimental observation and from FEA computation compared with the experimental values from the steady state propagation. [17]

12
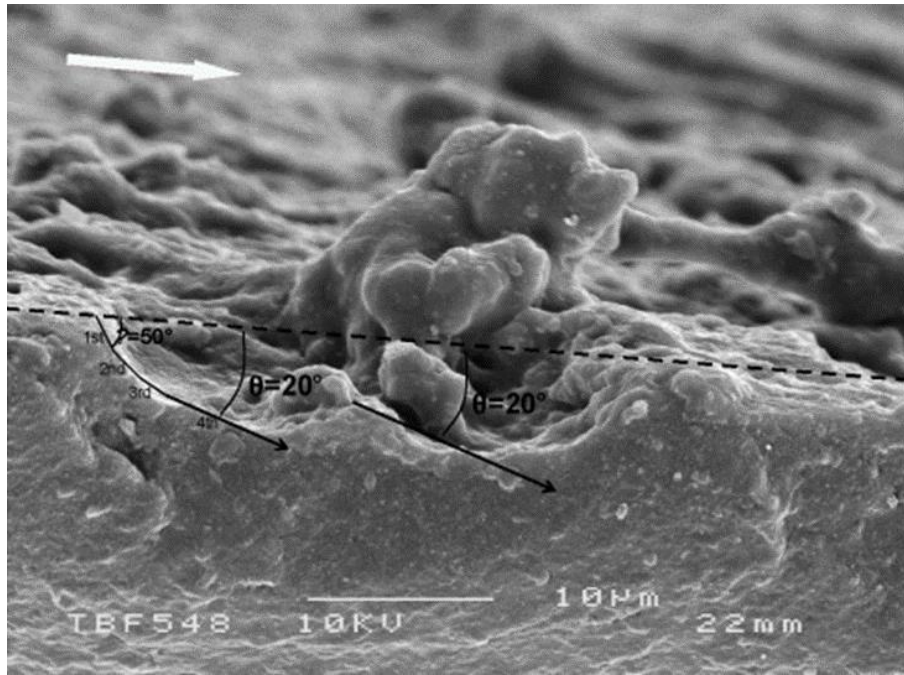
Figure 6. Initial cracks observed after 100 revolutions with a 20 N normal load. [17]

Chapter 2

Experimental methods

2.1 Test equipment introduction

2.1.1   UMT-3

UMT (Universal material tester), shown in the figure 7, can be applied to test the tribological properties of ferrous and non-ferrous metals, plastics, composites, different kinds of lubricants and the thin and thick coatings. Pin on disc, ball on disk, pin on V-block or disk on disk are the common test types of UMT. In this experiment, a pin-on-disk set-up is applied to conduct friction experiments under various conditions. The lower rotational motion drive rotates the lower disk. And the pin holder which can be used to keep the pin is attached to the contact suspension. The applied normal force is feedback controlled. The feedback control of the constant normal load is achieved by the normal-load sensor, which can provide feedback to the vertical motion controller and then adjust the upper pin's vertical position. The precise measurement of the normal load is in the range from milligrams to kilograms and the resolution is 0.00003% of the dull-scale. In addition, an electrical contact resistance sensor can be used to detect the contact between the lower disk surface and the upper pin.

The travel length of the upper vertical linear motion system is 150 mm and the lower rotational driver, which is controlled by a precision spindle, capable of speeds is from 0.001 rpm to 5000 rpm.

The control unit and the testing unit are the two basic systems. The control unit is used for the data acquisition and computerized motor control. The testing unit is applied to control the position of the test samples. It is consisted of the vertical positioning

system and a lateral positioning system. They are both computer motorized control. For the vertical positioning system, its maximum travel is 150 mm and the capable of speeds is from 0.001 to 10 mm/s. And for the lateral positioning system, the maximum travel is 75 mm and the capable of speeds is from 0.01 to 10 mm/s.

Figure 7. UMT-3 tribometer

2.1.2 Stylus profilometer

Profilometry is commonly applied to measure the volume of material removed from a worn surface. In our analysis, we use the VeecoDektak 150 profilometer, shown in the figure 8 below. Its vertical resolution is less than 1 nm and when using a stylus tip of 2 micrometers, it has a lateral resolution along the surface of approximately 1 micrometer. Its measurement range is up to six inches in dimension and four inches thick. In addition, its diamond-tipped L stylus can conduct the precise two dimensional profile with the stylus force range from 1 mg to 15 mg.
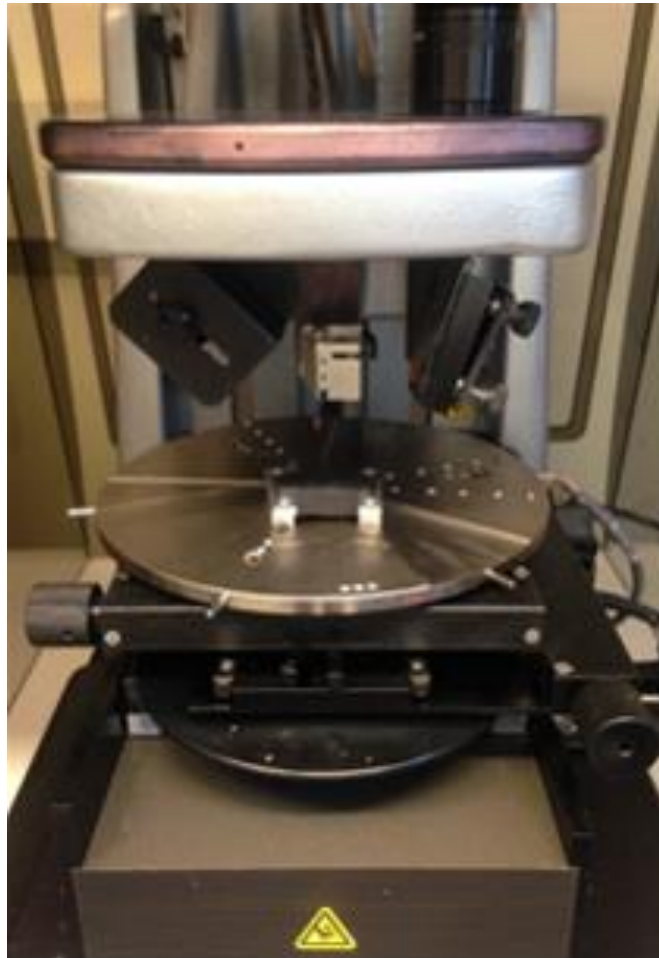
Figure 8. VeecoDektak 150 profilometer

It can provide researchers with the topography information of the wear scar, as well as the surface roughness. When we use the standard 2-D Dektak 150, the sample on positioning stage can be manually adjusted in the X and Y directions.

The Figure 9 below shows the architecture of the Dektak 150 system and how the system works. A Linear Variable Differential Transformer (LVDT) is applied, which is mechanically connected with the stylus. A custom-programmed scan file which has the information of scan length, time duration, speed and applied stylus force is used to control the whole scan process. The stylus moves on the lower sample surface and because of the surface texture, the stylus will move up and down to track the surface profile. The movement of the stylus caused the electrical signals which can be translated as the core position of the LVDT. Through the signal conditioning and A/D conversion, the position change is converted to the digital format data and stored in the computer memory.
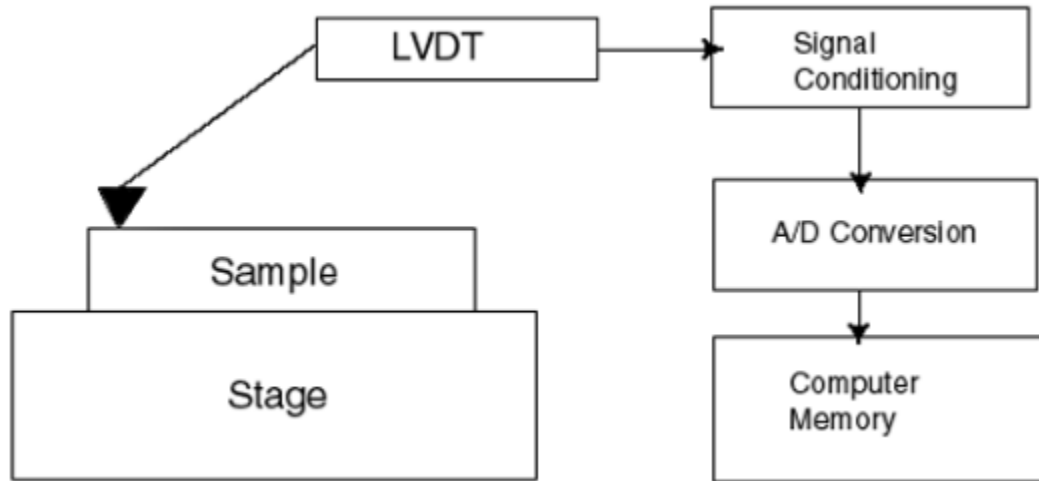
Figure 9. Block Diagram of the Dektak 150 Architecture [19]

2.2 Test samples

2.2.1 Rubber samples

According to the practical application of the experiment, four types of rubber with significantly different material properties were chosen to use. There are (1) soft rubber for SBR/NR mix, 60 duro, (2) hard rubber for SBR/NR mix, 80 duro, (3) new rubber for Butyl, 50 duro and (4) natural rubber for 100% NR, 65 duro. As the durometer (duro) is a measurement of rubber hardness, the new rubber is the softest one. NR refers to natural rubber, which is made from latex liquid, has good mechanical properties like strong tensile strength. Styrene-butadiene rubber (SBR) is a synthetic rubber with high filler loading capacity, crack-initiation resistance and abrasion resistance. SBR/NR refers to the blends of NR and SBR, NR is used to improve the mechanical properties of the synthetic rubbers such as tensile strength, resilience and fracture etc. And it is reported that

18

SBR/NR has an improved oxidative stability. [20] Butyl rubber is another type of synthetic rubbers has a very low resilience, which show a moderate resistance to abrasion and compression and an excellent performance for vibration damping and shock absorption application. [21]

The aim of this experiment is to see which kind of rubber has the best anti-wear properties when worn against composite materials like fiber-reinforced plastic (FRP) or Polyvinyl chloride (PVC). The samples of rubber of this experiment are larger and are approximately 14 mm x 30 mm x 8 mm, see figure 10 (a). They are cut from actual grommet material used in the practical application. The rubber samples are larger than the PVC and FRP samples and therefore their outer dimensions are not critical.

Table 1. Rubber Samples

Name	Material type	Hardness
Soft rubber	SBR/NR mix	60 duro
Hard rubber	SBR/NR mix	80 duro
New rubber	Butyl	50 duro
Natural rubber	100% NR	65 duro

2.2.2 Composite material samples

The contacting surfaces of the PVC samples are 5 mm x 10 mm and are the outer surface of the actual PVC pipe, see figure 10 (b) and 10 (c). Therefore these samples are convex on the contact and also 5.6 mm in thickness, which is the thickness of the PVC. The FRP samples are similar in geometry, but are thicker due to the larger size of the original FRP material (10mm).

The fiber-reinforced plastic (FRP) applied in this experiment is made of a polymer matrix reinforced with fibers such as glass, carbon, aramid or basalt. It is widely applied when the weight saving is needed. It is also a good substitute to steel or aluminum products because of the cheaper, faster and easier manufacturing. The other good quality is its structure enhancement. For the glass fibers reinforcing material, the strength, elasticity and heat resistance will be improved relative to the polymer material, while for the carbon and aramid fibers reinforced, the tensile strength and compression strength properties will get better.

For composite materials, whether the mechanical properties of the fiber-reinforcement plastic is improved or not depends on the properties of both the fiber and matrix, the ratio of each volume, the length of the fiber and their orientation[22]. For the FRP, by specifying the orientation of the fibers, the strength or other specific properties can be improved to fit a particular requirement. For example, with the glass fiber reinforcement materials, if the fiber's orientation is parallel to the direction of the applied force, it will get the best deformation resistance, while if the orientation of the fiber is perpendicular to the applied force, the enforcement will be weak. In addition, the strength and the elasticity properties of the composite material will be less than the matrix material.

Polyvinyl chloride, commonly abbreviated PVC, is the third-most widely produced synthetic plastic polymer, after polyethylene and polypropylene. [23] PVC has a high hardness and good mechanical properties in general. With the increasing of temperature the mechanical properties are decreased while with the increasing of

molecular weight, they are enhanced. It has a wide range of application due to its low cost, workability and good biological and chemical resistance.

Table 2. Material Pairs

Rubbers	Hard Rubber	Soft Rubber	New Rubber	Natural Rubber
Harder composite materials	FRP	FRP	FRP	FRP
	PVC1	PVC1	PVC1	PVC1
	PVC2			PVC2
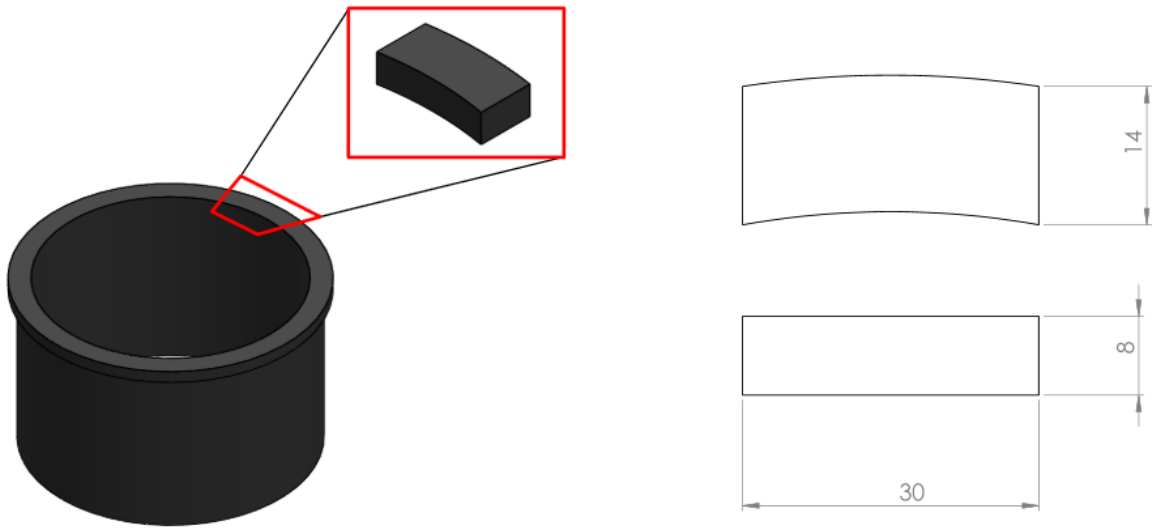
(a) Rubber sample
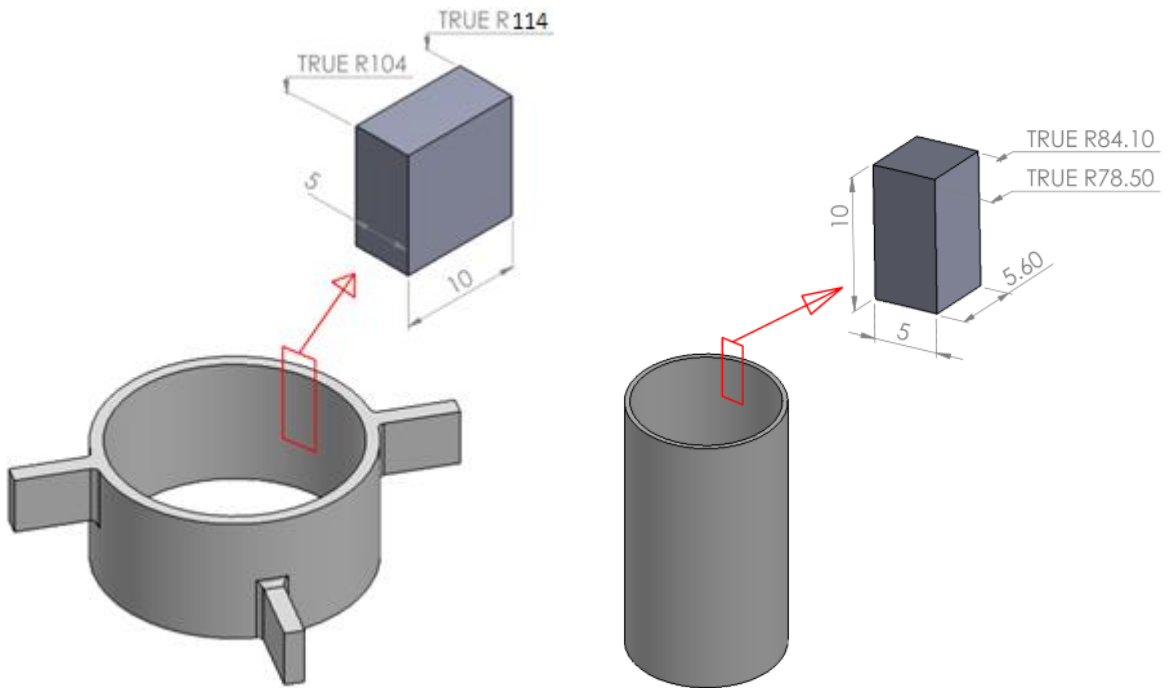
(b) FRP sample   (c) PVC sample

Figure 10. Schematic of test samples

2.2.3 Media environments

According to the practical application, three test lubricant conditions – air, water, and slurry, were applied to conduct the experiments. The slurry used in this experiment is a mixture of an insoluble substance, as cement, clay, coal, limestone, or lime with a liquid, like water. For the slurry, the particles may settle during the test, and therefore an agitating stirrer (see Figure 11) was designed to keep the solid particles mixed in the slurry.
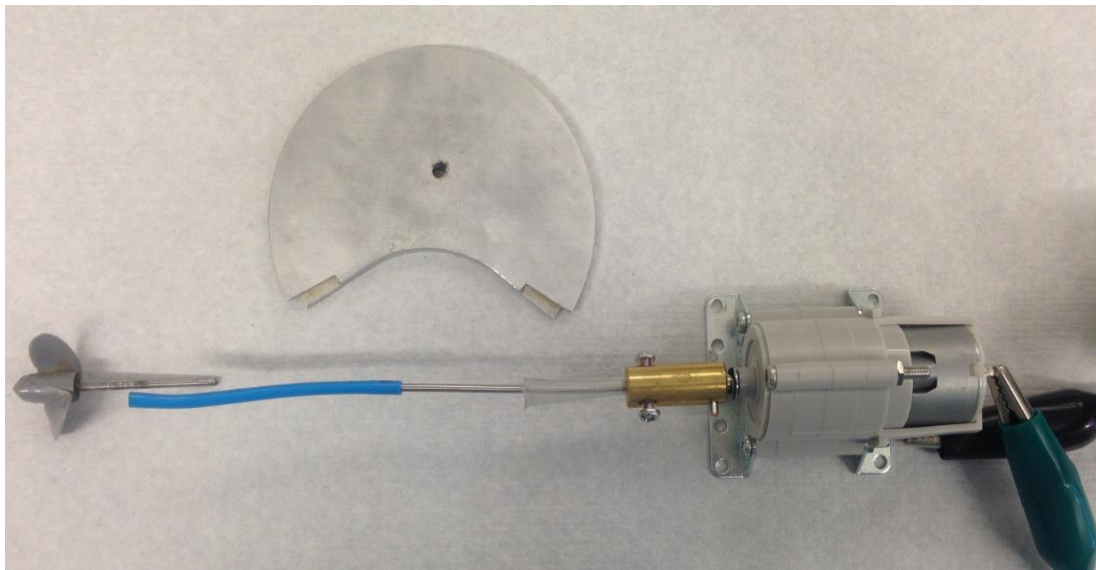
Figure 11. Schematic of the stirrer

2.3 Experimental set-up

2.3.1 Test design

The pin-on-disk apparatus of a Bruker UMT (Universal Material Tester) Multi-Specimen Test System manufactured by Bruker was applied to study the tribology properties of different kinds of rubber specimens contacting PVC or FRP. The test method involves a lower specimen made of the rubber that is reciprocated in a sliding motion against a rectangle shaped upper PVC or FRP sample under a prescribed set of conditions. During the test, the UMT can monitor the actual dynamic normal load, friction force and the friction coefficient.

Figure 12(a) shows the schematic view of the test rig we used to conduct experiments. Detailed schematics of the test rig parts are also included in Appendix 1 of this thesis. The upper PVC or FRP samples are held in the pin holder which is mounted on the UMT force sensor. The force sensor can control the normal load applied to be nearly constant at 100 N. The reservoir, which can hold and fix the lower rubber sample and contain slurry fluid or water, is mounted on the UMT rotary drive. The section view of the test ring is shown in Figure 12(b). The rotary drive is controlled through the PC and maintains the prescribed reciprocating motion of the rubber specimen. The average velocity during sliding is set to 120 rev/min and the reciprocating angle is 0.04π. Thus, the average sliding distance of rubber against the PVC or FRP is 2.2608 mm per a cycle at 140 cycles for per minute. The duration for each test is 3 hours. Then the total sliding distance for each test is 56.97 m.

Mounts on the UMT
Force Sensor

Mounts on the UMT
Rotary Drive
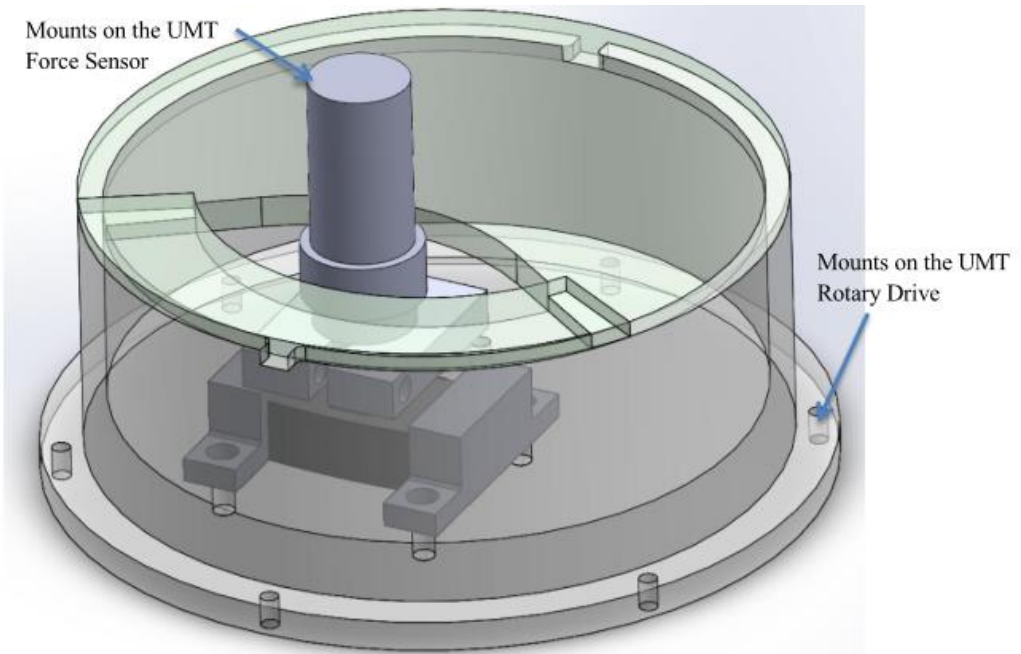
(a)
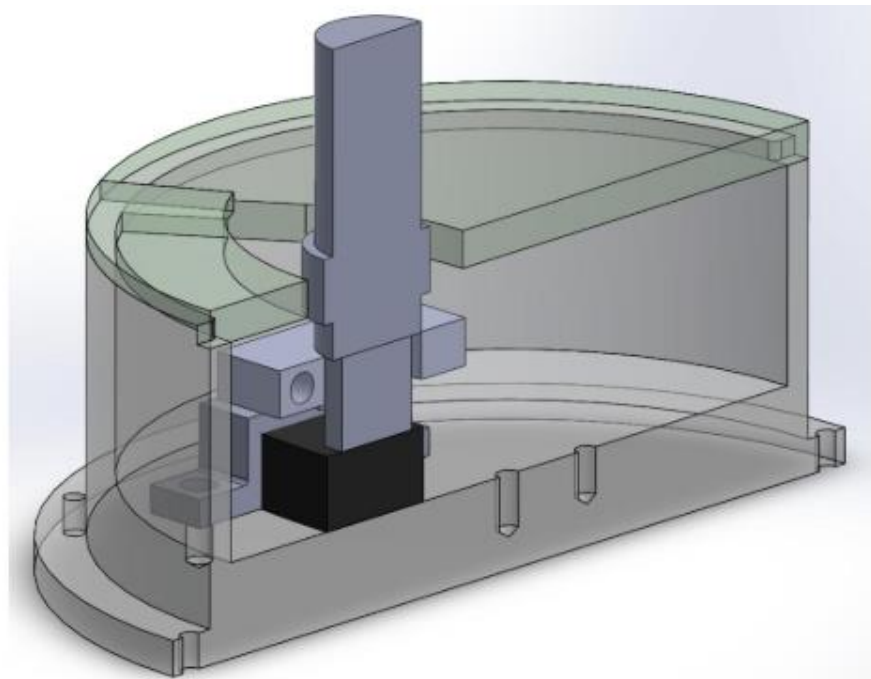
(b)

Figure 12. Designed test rig to assess the contact wear

Figure 13. Test setup parts

Test setup parts are shown in Figure 13. A clamp holds the rubber sample to the base of the reservoir. The opposite contacting surface of the FRP and PVC samples are held by a custom fixture that is attached to the vertical stage and force sensors of the UMT test machine. From Figure 14, it is shown that the PVC/FRP samples are held in the slot of the upper holder which is fixed in the UMT by a bolt, so it cannot move up and down. And the clamp around the slot is held with a pin so the samples cannot slip. Again, schematic drawings of all of these items are available in the Appendix 2.
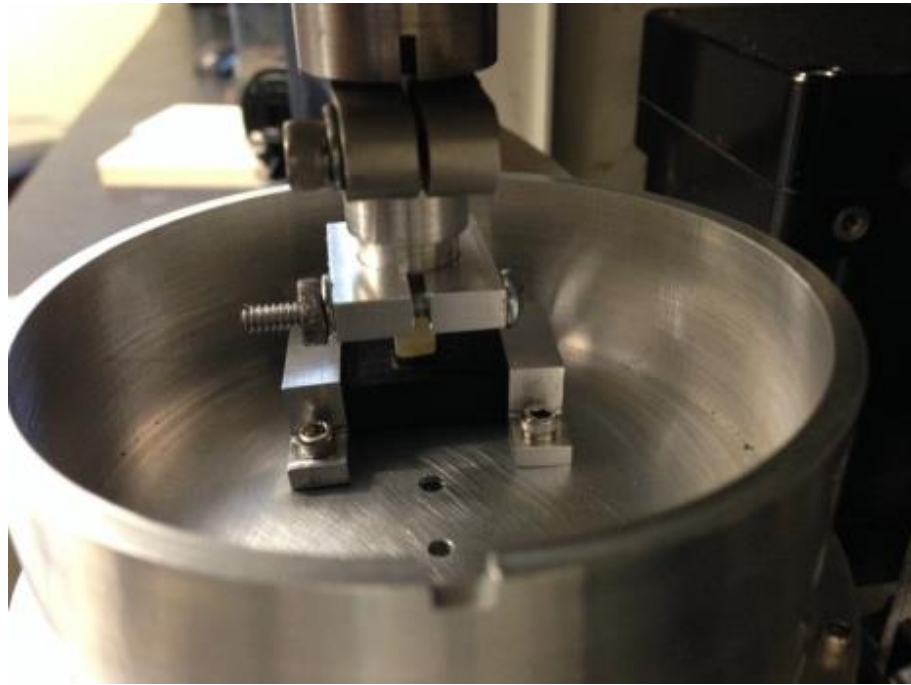
(a)
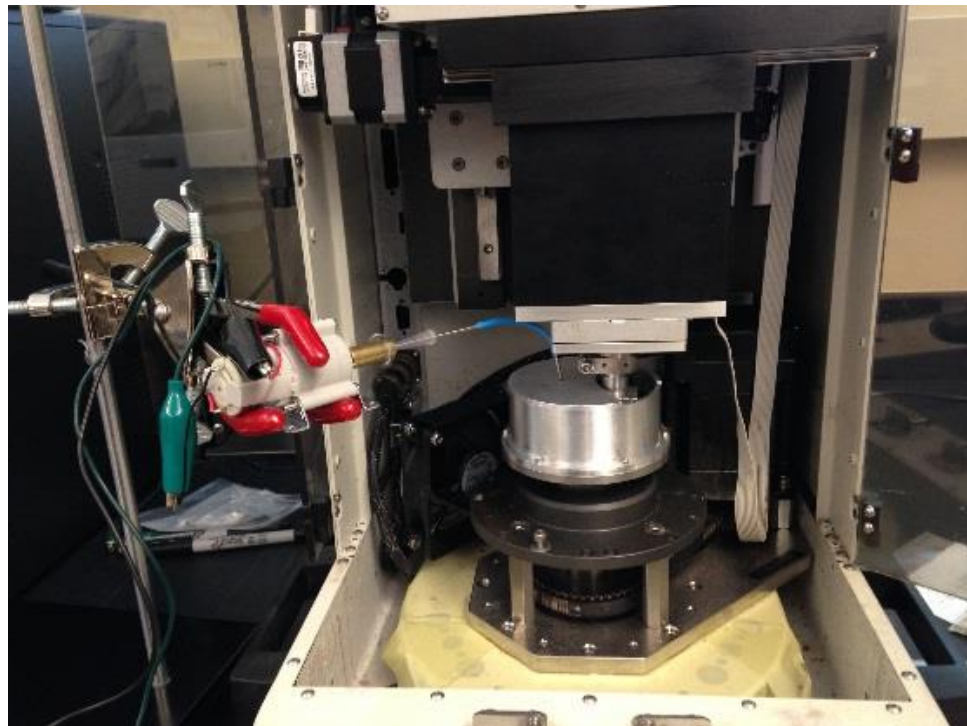
(b)

Figure 14. Test setup assembly

2.3.3 Test schedule

For each single test, a combination of two individually selected material types, which are a rubber material and a mating surface material such as PVC1, PVC2 or FRP, are immersed in a single media, such as air, water or slurry. In order to obtain an understanding of the repeatability and scatter of the results, the tests were repeated three times for each material pair. This resulted in the test matrix shown in Table 3.

Table 3. Test Matrix

Test	Material 1	Material 2	Media
1	PVC	Soft Rubber (SBR/NR mix, 60 duro)	Air
2	PVC	Soft Rubber (SBR/NR mix, 60 duro)	Water
3	PVC	Soft Rubber (SBR/NR mix, 60 duro)	Slurry
4	FRP	Soft Rubber (SBR/NR mix, 60 duro)	Air
5	FRP	Soft Rubber (SBR/NR mix, 60 duro)	Water
6	FRP	Soft Rubber (SBR/NR mix, 60 duro)	Slurry
7	FRP	Hard Rubber (SBR/NR mix, 80 duro)	Air
8	FRP	Hard Rubber (SBR/NR mix, 80 duro)	Water
9	FRP	Hard Rubber (SBR/NR mix, 80 duro)	Slurry
10	PVC1	New Rubber (Butyl, 50 duro)	Slurry
11	PVC1	Hard Rubber (SBR/NR mix, 80 duro)	Slurry
12	PVC2	Hard Rubber (SBR/NR mix, 80 duro)	Slurry
13	FRP	New Rubber (Butyl, 50 duro)	Air
14	FRP	New Rubber (Butyl, 50 duro)	Water
15	FRP	New Rubber (Butyl, 50 duro)	Slurry
16	PVC1	Natural Rubber (100% NR, 65 duro)	Slurry
17	PVC2	Natural Rubber (100% NR, 65 duro)	Slurry
18	FRP	Natural Rubber (100% NR, 65 duro)	Slurry

2.3 Worn surfaces analysis methods

2.4.1 Wear analyses for rubber samples

A VeecoDektak 150 profilometer is employed to measure the volume of material

removed from the worn rubber surface. In our analysis the measurement provides us with

a profile of the worn surface of the rubber, the PVC and FRP (although the wear of theses

samples appears minimal). In order to obtain reliable results, six profiles, three in the

sliding direction and three perpendicular to the sliding directions, were measured for each

worn surface as shown in the Figure 15 and 16.

The material of volume removed can be assessed from the depth of the wear

scars. In the current work several quantities were calculated from the measurements 1)

the maximum wear depth including cracks, 2) the maximum wear depth without cracks,

3) the average wear depth without cracks. These were all calculated in both the sliding

and perpendicular directions to compare the wear for different types of rubber. The

standard deviation for each value was calculated to show the statistical repeatability of

the wear measurements. Basically, two sets of the data were chosen from the three tests.

Maximum wear depths without cracks calculated the single largest wear depth without

considering the depths of cracks for each sample and chose the largest number from

them. Then 12 numbers in both directions and 6 numbers in the sliding directions were

used to obtain the standard deviations. In addition, the worn surfaces were qualitatively

analyzed using an optical microscope to see the details of the contact surfaces of the

rubber.
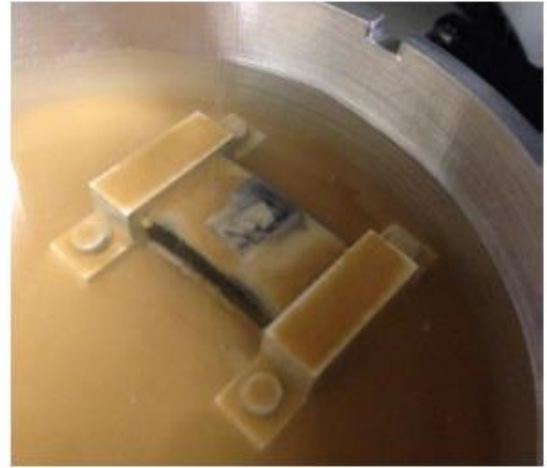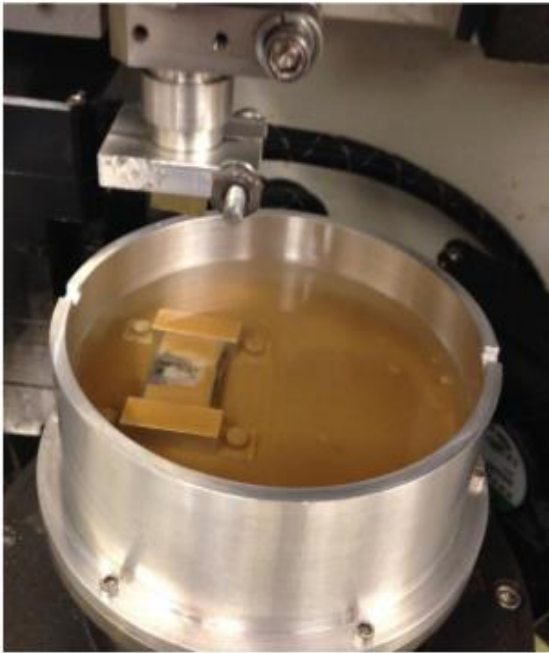
(a) Test for slurry case

Contact region
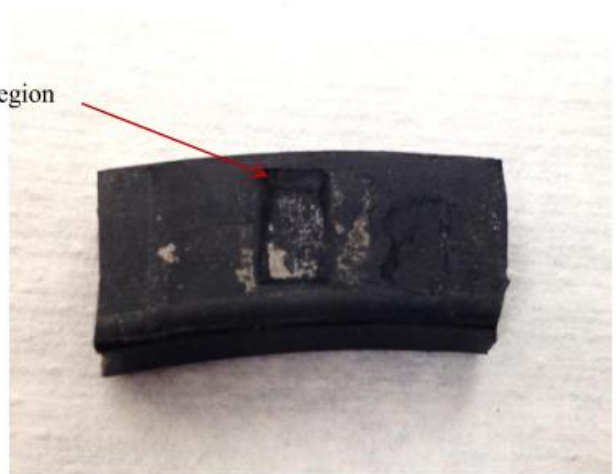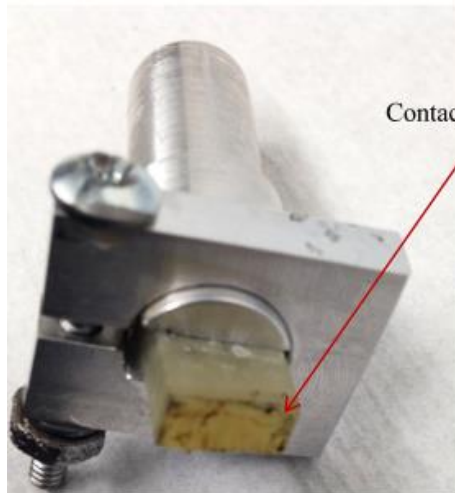
(b) Samples after the test

Figure 15. Test observation

Sliding directions

(a)

(b)
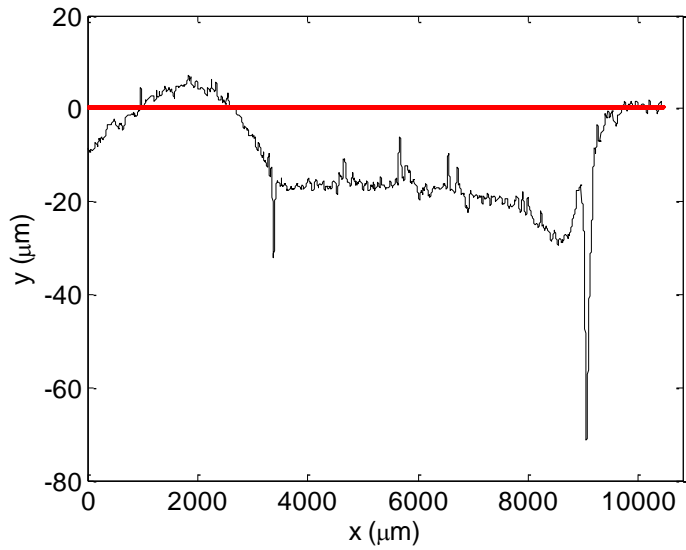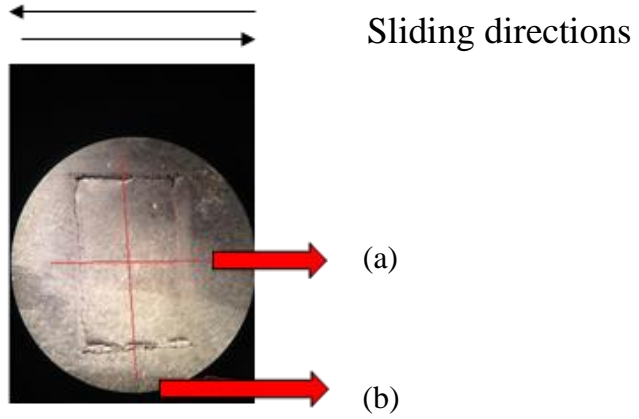
(a) Profile in sliding direction
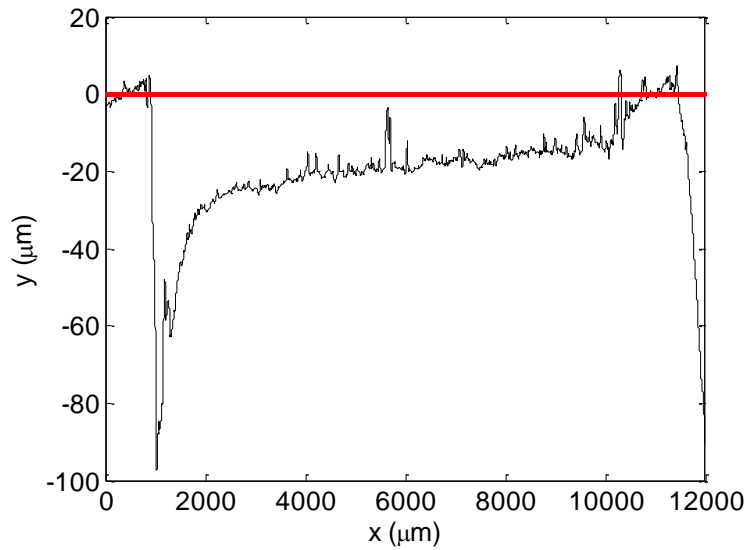
(b) Profile perpendicular to sliding direction

Figure 16. Surface profiles measured using profilometry

2.4.2 Wear measurement of FRP and PVC

For the small hard PVC and FRP samples, measurement of the mass before and after each slurry test were performed by using a highly sensitive precision analytical scale (see Figure 17). The analytical scale has an accuracy of 0.01mg. However, the change in mass due to wear on the PVC1, PVC2 and FRP are usually small. Therefore we also measured the surface roughness of the PVC1, PVC2 and FRP samples by using the profilometer before and after each slurry test to observe any changes in the roughness during each test. This is not the best method to characterize wear and therefore was not performed on the earlier tests. Such changes could indicate that the surfaces are indeed wearing, but at a very slow rate.
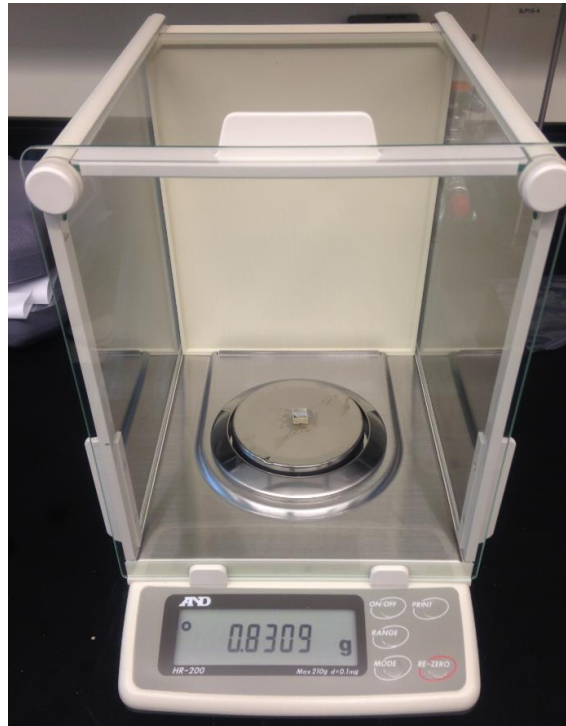
Figure 17. Analytical scale

Chapter 3

Experimental results of wear

3.1 Wear depths of different kinds of rubber measured in both directions

3.1.1 Hard rubber against FRP tests

As described in the previous sections, sliding tests were conducted for hard rubber and FRP material pairs in air, water and slurry. Three tests were run for each lubricant condition. The resulting wear depths measured in both directions are shown below in Figure 18. The error bars show the standard deviation of the data.
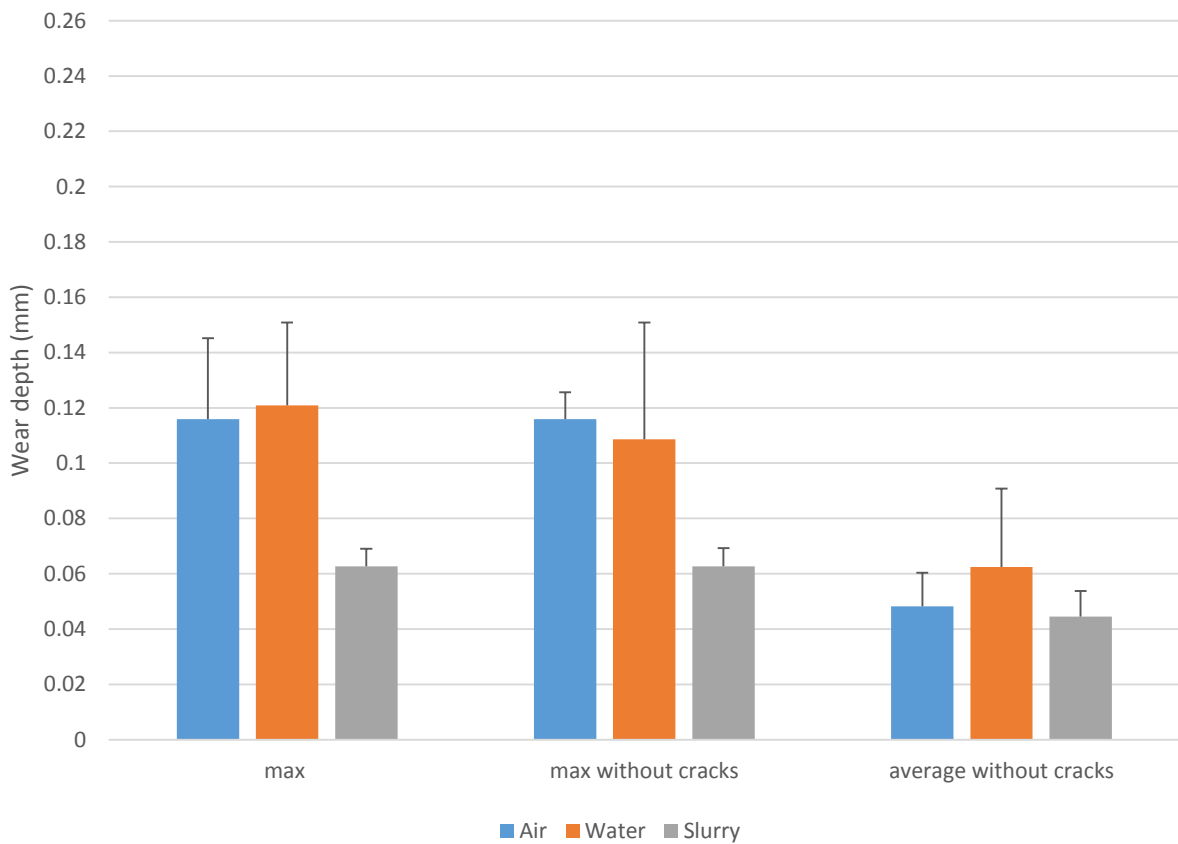
Figure 18. Wear depths for hard rubber against FRP measured in both directions

From Figure 18, it is observed that in the water and slurry conditions for the hard rubber against FRP, the wear depths were decreased. And for the slurry tests, the effect of the cracking is statistically less but the overall wear did not decrease very significantly. The particles in the slurry may be reducing the friction between the surfaces which allows for more relative motion with less tangential loading. The tangential loading could be tearing the rubber. Note that tearing and cracking are the same mechanism here. Cracking is a possible failure mechanism and should be a concern. It should also be noted that if the maximum equals the maximum without cracks, then no obvious cracking was observed.

3.1.2 New rubber against FRP tests
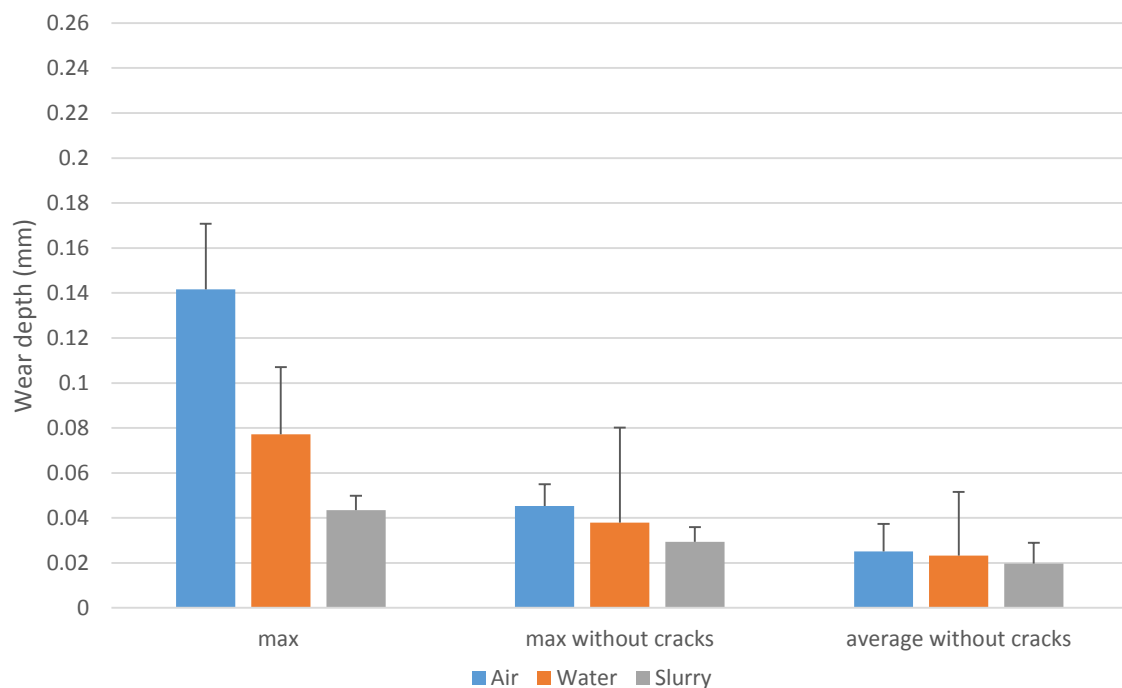
Figure 19. Wear depths for new rubber against FRP measured in both directions

Sliding tests were conducted for new rubber and FRP material pairs in air, water and slurry. Three tests were run for each lubricant condition. The results of wear depths measured in both directions are shown below in Figure 19. The slurry has a positive effect on decreasing the wear. However, once cracks are removed, the difference in the wear between the three samples appears to be minimal.

3.1.3 Soft rubber against FRP tests

Sliding tests were conducted for soft rubber and FRP material pairs in air, water and slurry. Three tests were run for each lubricant condition. The results of the wear depths measured in both directions are shown in Figure 20. For this pair, cracking again appears to contribute to a large portion of the surface wear and damage. In addition, it appears that the slurry may actually increase the wear for this case.
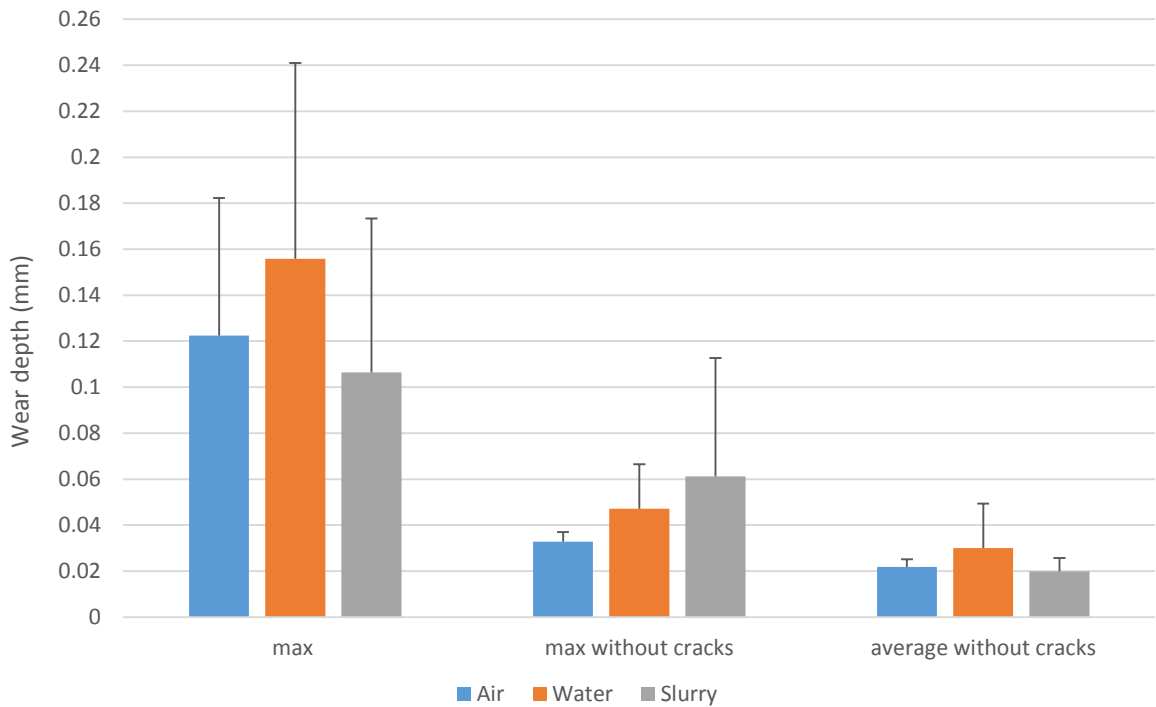
Figure 20. Wear depths for soft rubber against FRP measured in both directions

3.1.4 Soft rubber against PVC1 tests

Sliding tests were conducted for soft rubber and PVC1 material pairs in air, water and slurry. Three tests were run for each lubricant conditions. The results of wear depths measured in both directions are shown in Fig. 21. For the soft rubber against PVC, the cracking does not appear to be as severe as against FRP. This is probably due to there being less friction between the surfaces that allows them to slide with less stress that may cause ripping or cracking of the rubber. The slurry again here appears to decrease the wear slightly. In addition, the results of average without cracks are more stable and repeatable.
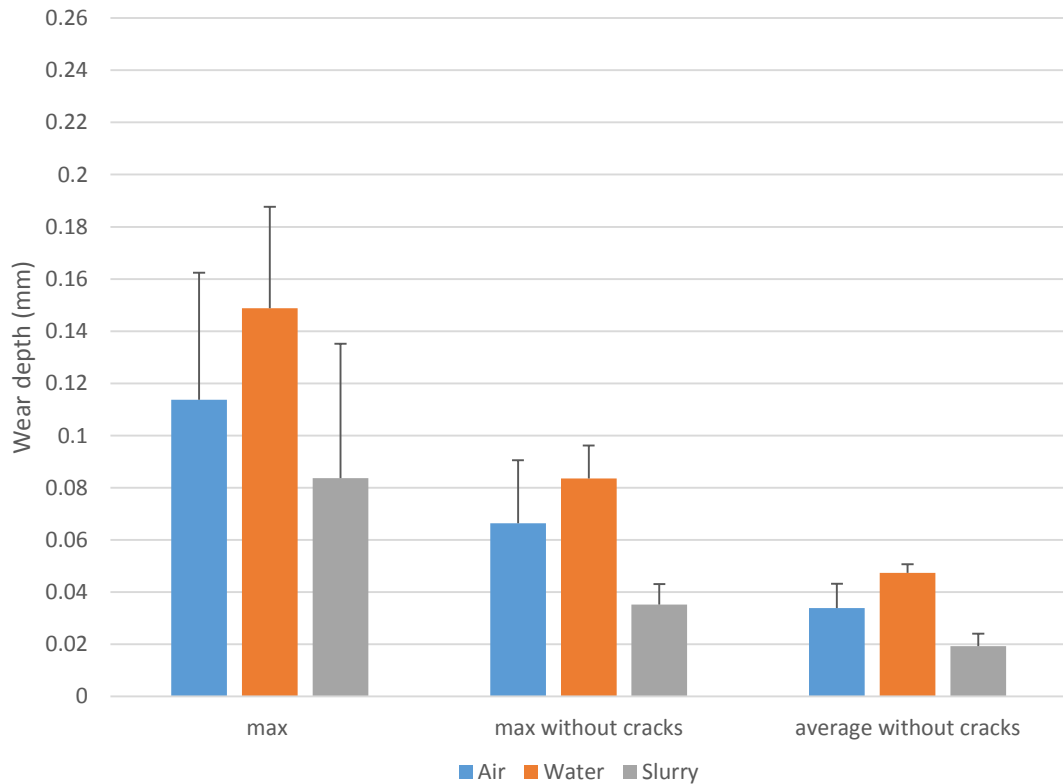
Figure 21. Wear depths for soft rubber against PVC1 measured in both directions

3.2 Wear depths of different kinds of rubber measured at sliding direction

Figure 22 to Figure 26 show the wear depths of different kinds of rubber we measured in the sliding direction. This differs from the earlier results in that wear was only calculated in one direction, by taking only a roughness profile in the direction of sliding. Since there appeared to be more cracking on the edges, this removed that cracking from the measurements. From this data, we can see that overall, the new rubber seems to be the best for anti-wear.
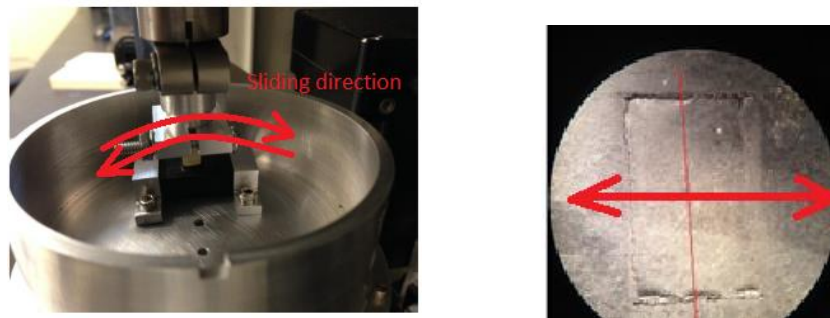
Figure 22. Schematic drawing of sliding direction
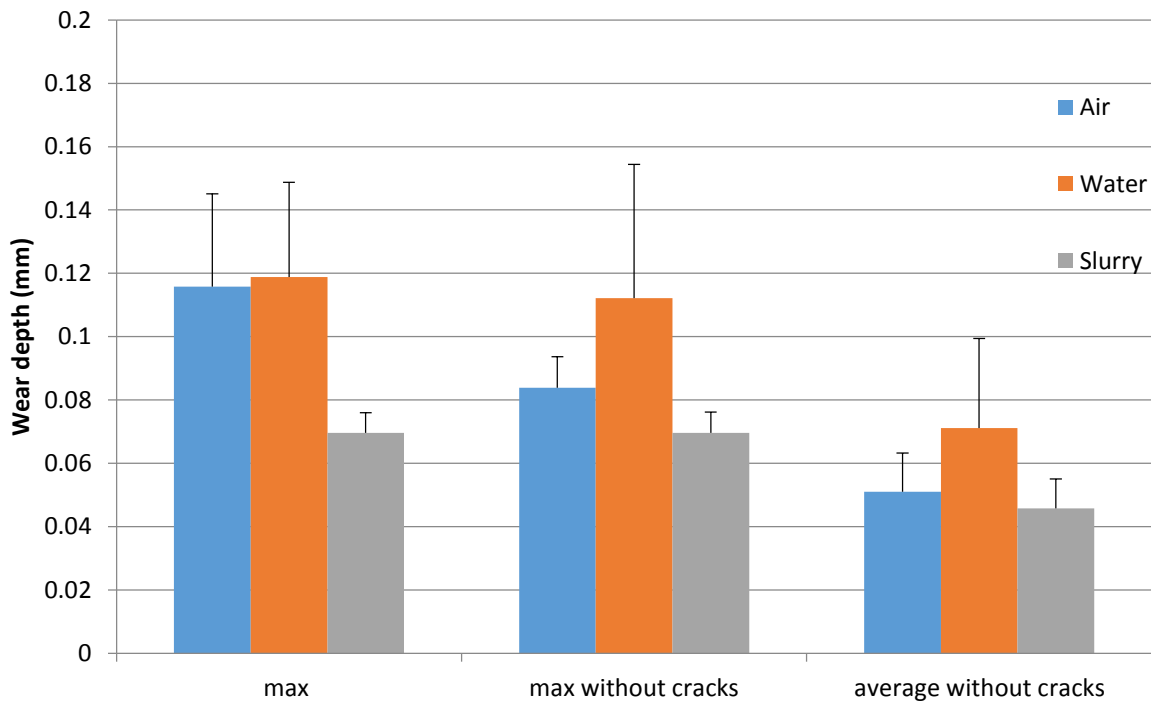
Figure 23. Wear depths measured at sliding direction for hard rubber against FRP
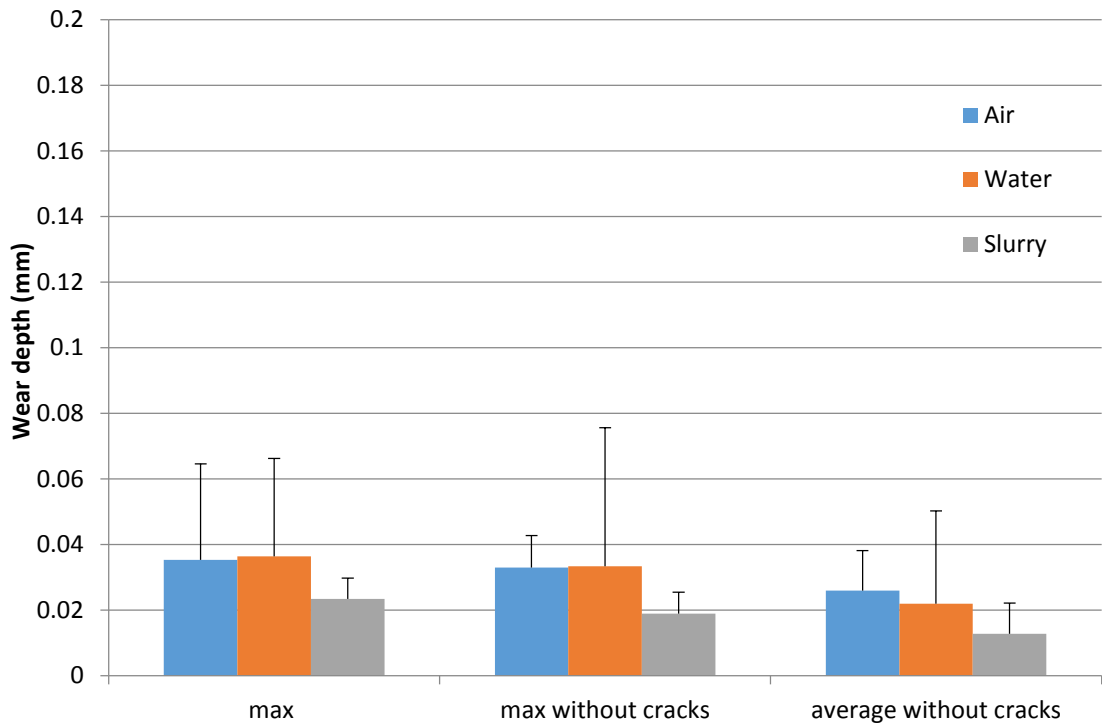
Figure 24. Wear depths measured at sliding direction for new rubber against FRP
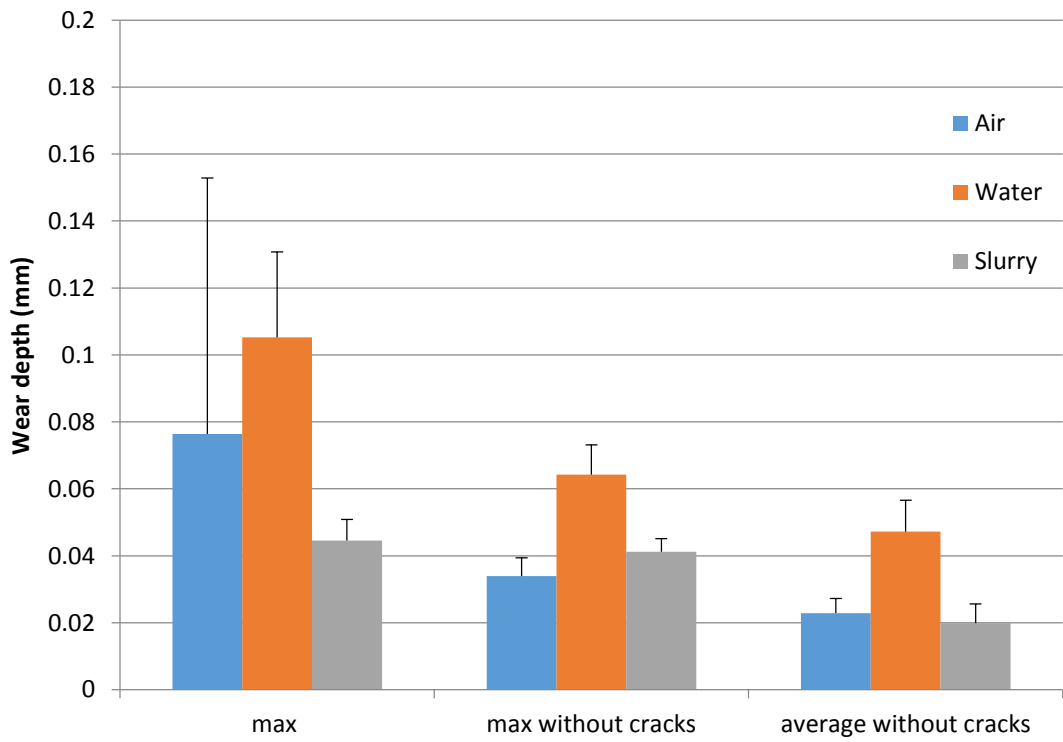
Figure 25. Wear depths measured at sliding direction for soft rubber against FRP
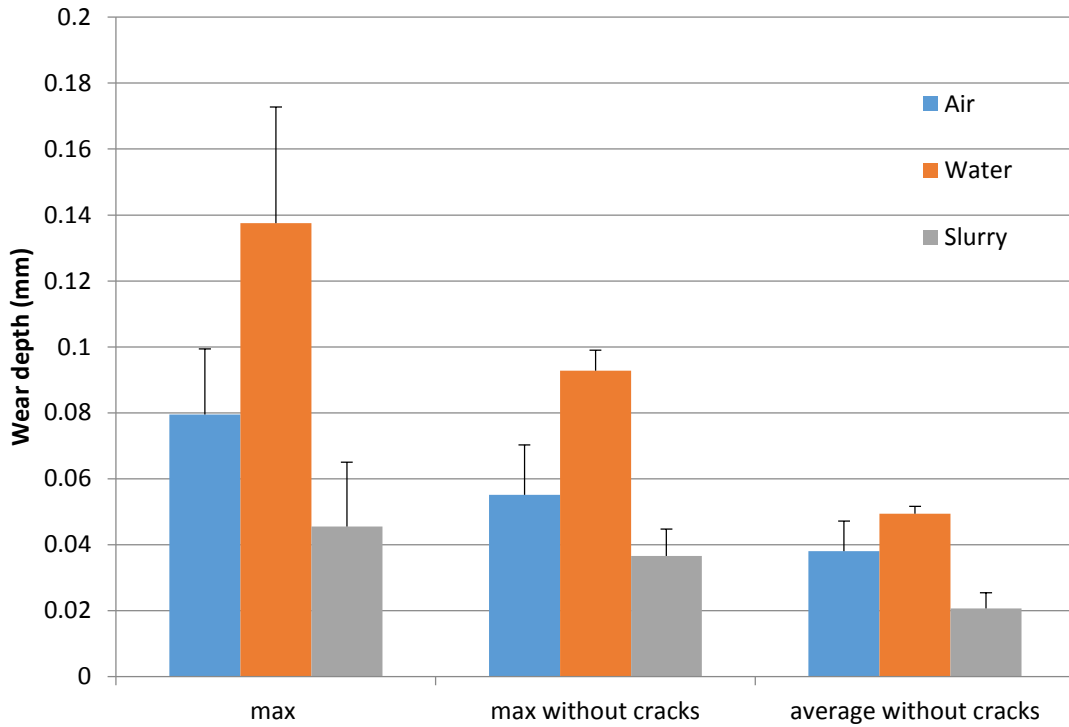
Figure 26. Wear depths measured in sliding direction for soft rubber against PVC1

3.3 Wear depths of different kinds of rubber against FRP

A set of slurry tests were run for each type of rubber against FRP to make a clear comparison. Wear depths were measured in both the sliding direction and the direction perpendicular to sliding in the slurry tests. The results are shown in Figure 27. New rubber has the smallest wear depth in both directions when in contact against FRP in the sliding tests. However, natural rubber also has relatively low values, but there appears to be more cracking for natural rubber. The hard rubber appears to have more overall wear but less of a contribution from cracking. In contrast, the soft rubber appears to have a larger contribution from cracking. This is probably due to the different types of rubber having different mechanical properties, such as elastic modulus, friction, and strength.

Nonetheless, new rubber and natural rubber both appear to have significantly less wear and damage than the soft and hard rubber samples.
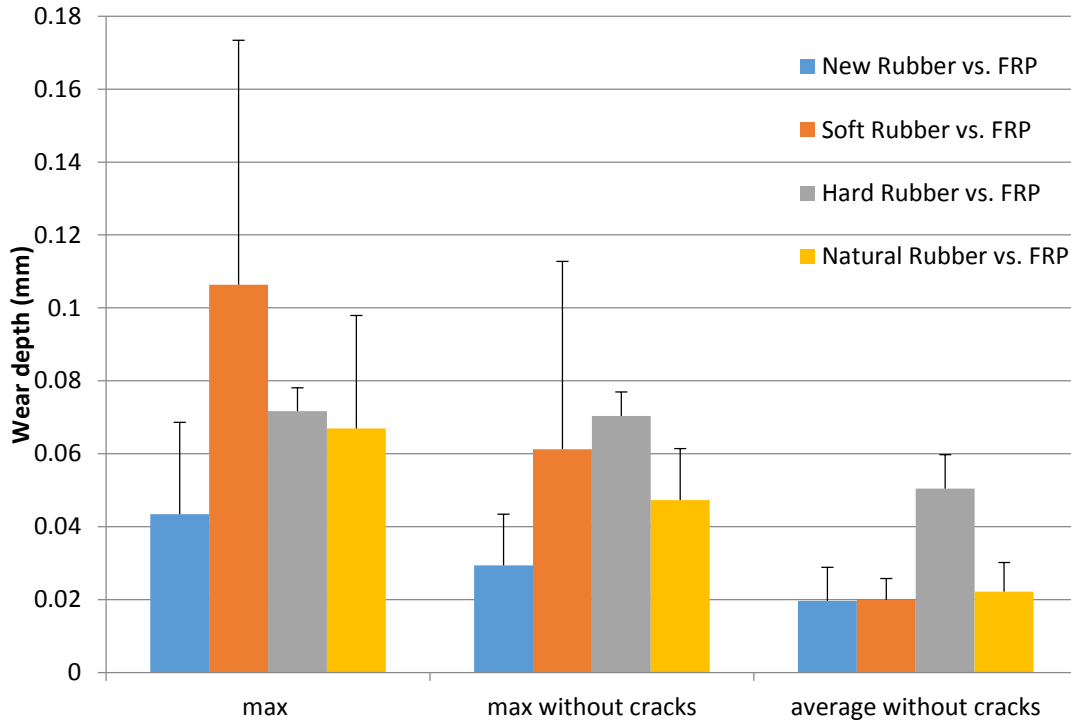
Figure 27. Wear depths of different kinds of rubber against FRP in the slurry

3.4 Wear depths of different kinds of rubber against PVC

Tests of different types of rubber against two types of PVC were also performed and compared. The wear depths were measured in both directions in these slurry tests as noted previously.

From the Figure 28, we can see that the natural rubber has the least wear for the PVC tests in slurry compared with all the other kinds of rubber. The natural rubber against PVC1 also appears to have slightly less wear than against the PVC2. However,

this is reversed for the hard rubber. Since these differences are relatively small, overall the type of PVC does not appear to be critically important.

Here it appears that a large portion of the damage in the natural rubber is due to tearing and cracking. In contrast, the wear for the new rubber has less of a contribution from cracking. Cracking and tearing of the rubber should be a concern as it could cause eventual failure of the rubber.
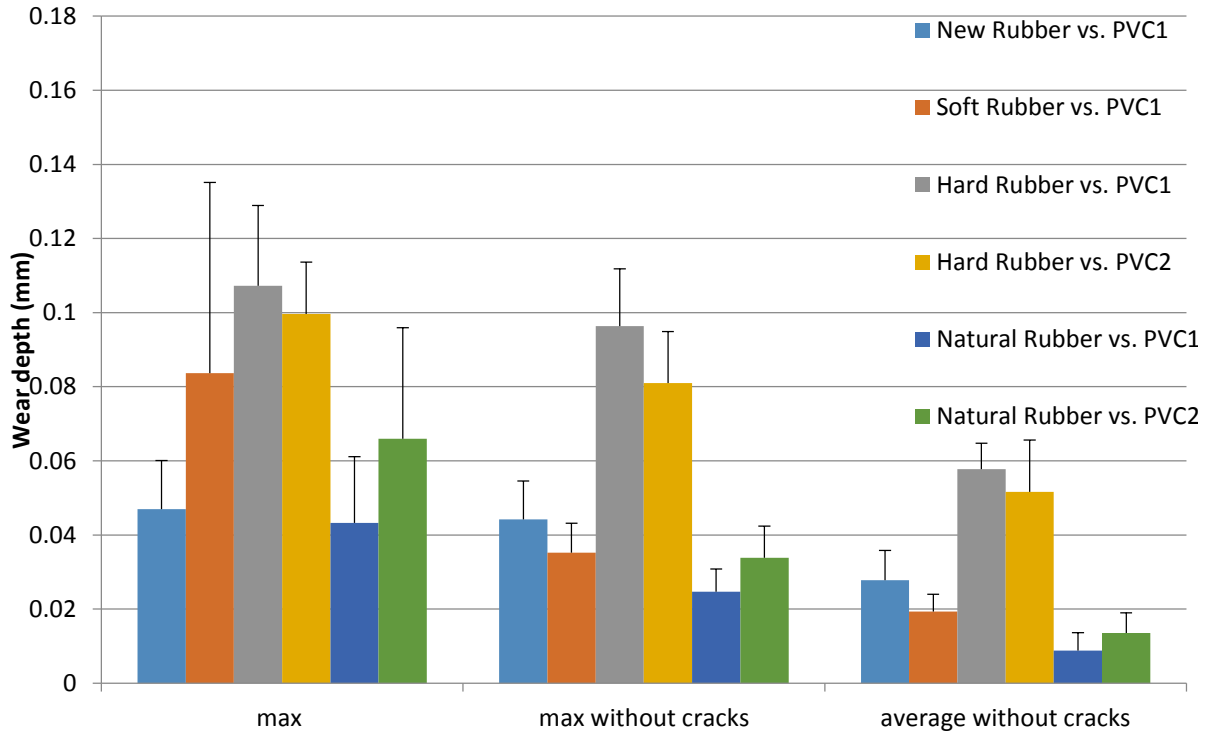
Figure 28. Wear depths of different kinds of rubber against two different PVC material formulations in slurry

3.5 Wear depths of different kinds of rubber

3.5.1 Wear depths of different kinds of rubber in both directions

All the results of the rubber tests in the slurry are shown in Figure 29 below on a combined plot to allow for direct visual comparisons. The new, soft, and natural rubber all appear to have good average wear, but the soft and natural rubber both appear to have significant cracking. Overall the new rubber appears to show the best performance, followed by closely by the natural rubber. The effect of the type of PVC and FRP does not appear to be a statistically significant factor.
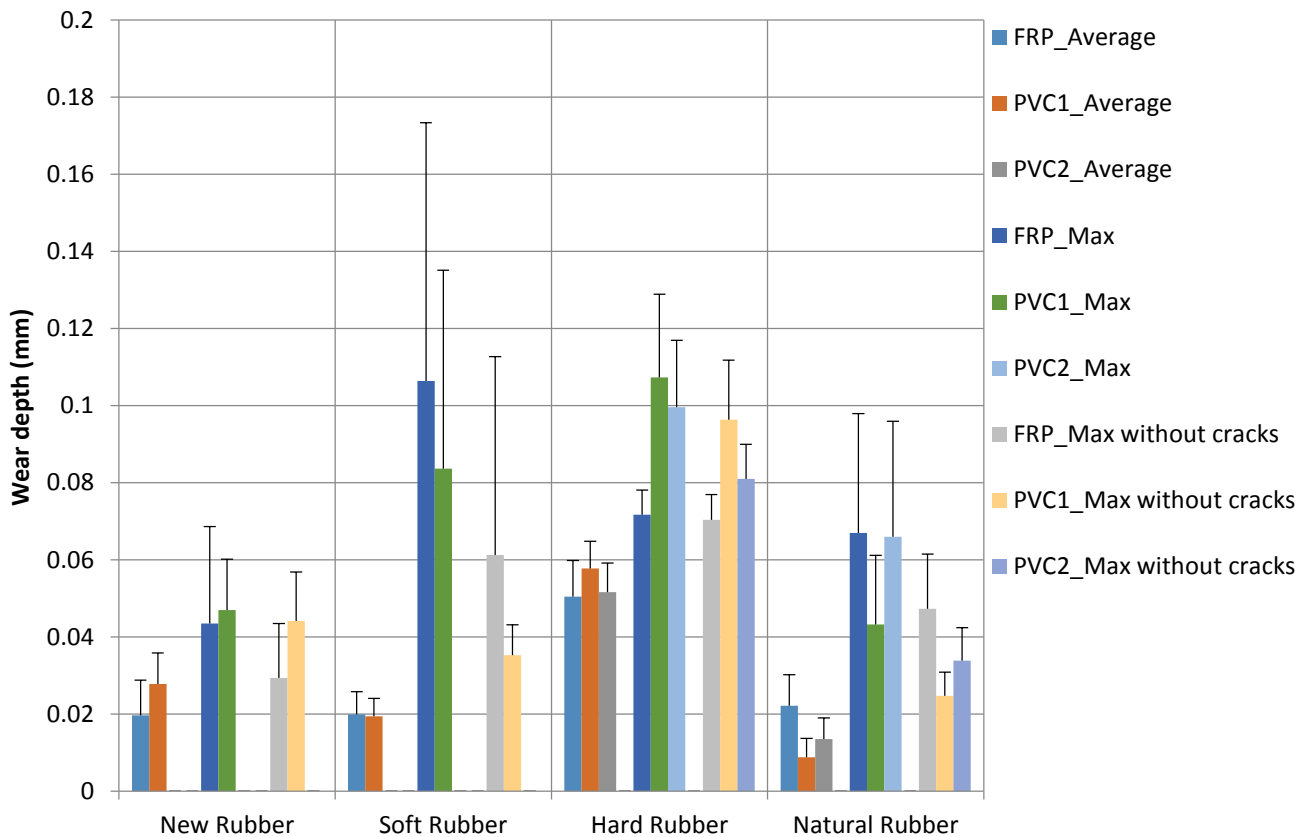
Figure 29. Wear depths of rubber in both directions in the slurry

3.5.2 Wear depths of different kinds of rubber in sliding directions only

       The results are now separated into only those in the sliding direction, since the cracking usually appears to occur mostly parallel to the sliding direction (i.e. a profile perpendicular to the sliding direction will measure it). Therefore, as expected, except for the hard rubber, the effect of cracking is reduced by only considering the profile in the sliding direction.
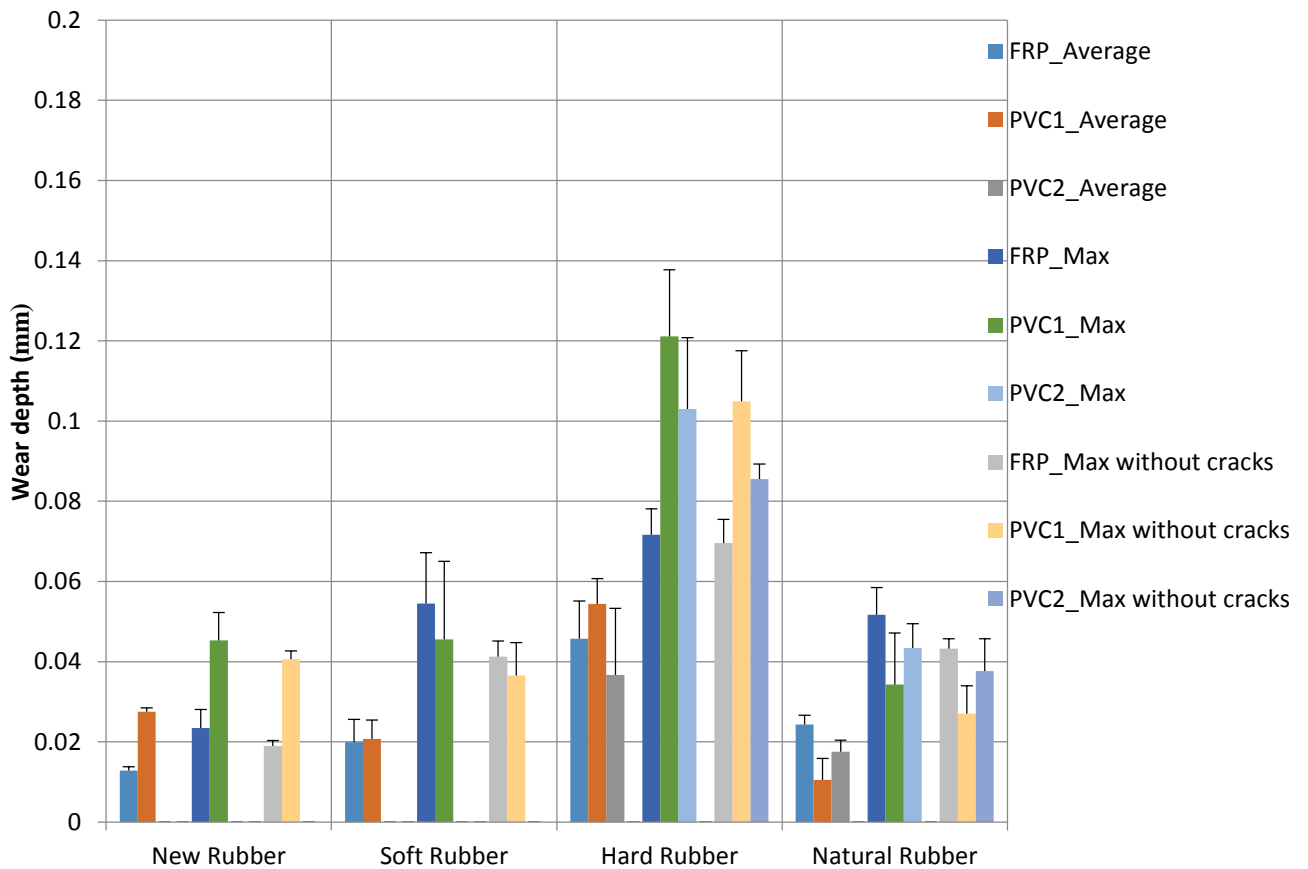
Figure 30. Wear depths of rubber in sliding direction only in the slurry

The Figure 30 shows that new rubber has the best anti-wear performance in this direction as well. However, the natural rubber also shows very good properties against PVC and for the averaged wear. The averaged wear for the soft rubber also seems to be very good, but cracking seems to be a major issue for that material. Hard rubber is clearly the least desirable material. The differences between the PVC types and FRP also appear to be statistically insignificant compared to the influence of the type of rubber.

3.6 Visual analysis of worn rubber surface

3.6.1 Typical worn surfaces for rubber against FRP

Photographs of typical samples were taken in order to allow for visual analysis and confirmation of the quantitative measurements. The lighting is slightly different in the photographs which can cause the appearance of discoloration. As labeled in Figure 31, the sliding direction of the rubber samples is in the vertical orientation.
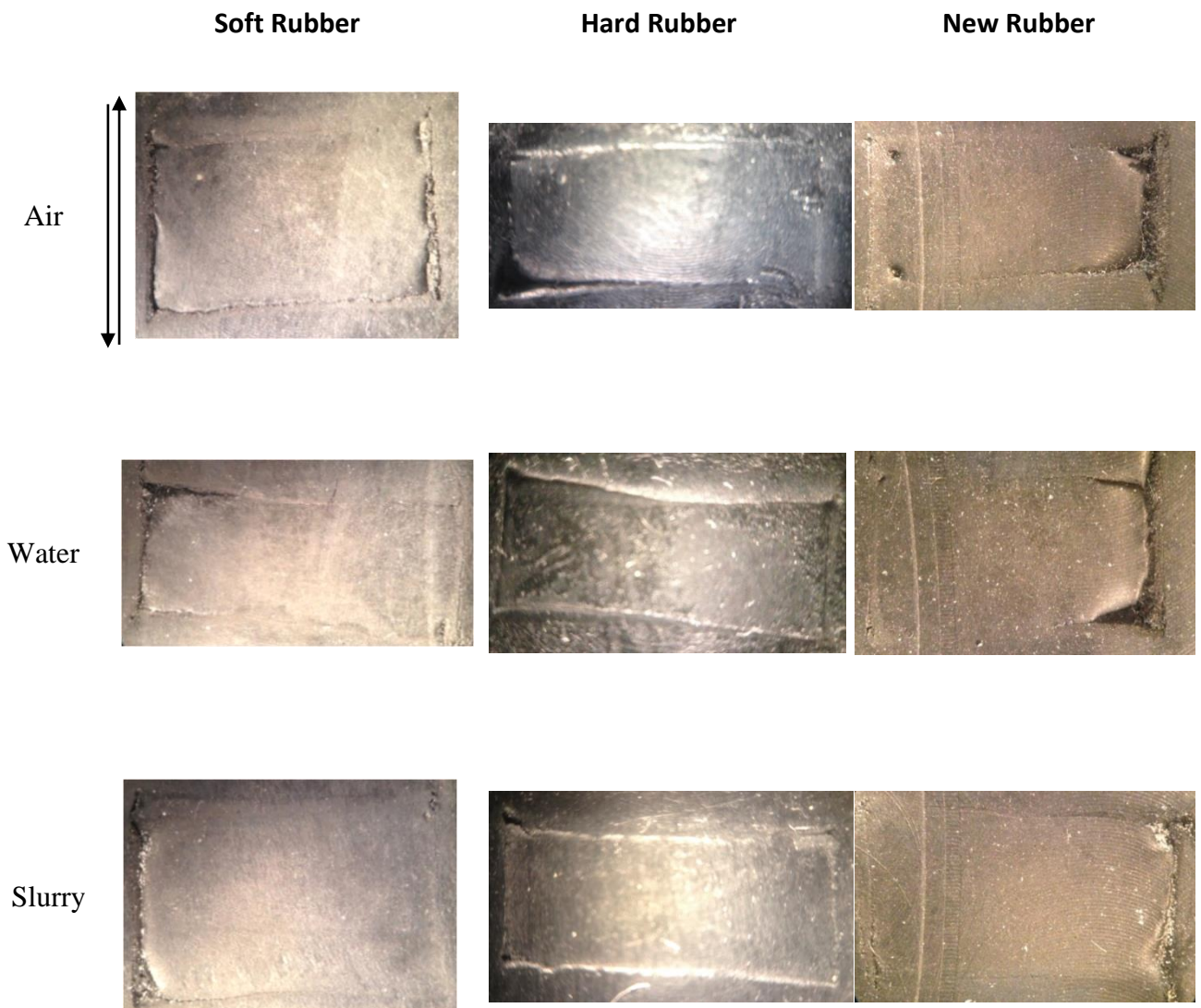
Figure 31. Worn surfaces of soft rubber, hard rubber and new rubber in air, water and slurry against FRP

From the worn surface pictures in Figure 31, there are wear and cracks on the edges of the contact surfaces. The cracks are especially significant for soft rubber. There are cracks for the new rubber samples on the edges of the sliding directions but the wear is not obvious. In the samples tested in the slurry, one can also notice the presence of a few solid particles of dried slurry on the surfaces, and especially in the cracks. This can show that slurry deposited and influenced the rubber wear when the upper samples contact and slide against the rubber. The slurry samples appear to possess slightly less cracks. Overall the visual inspection confirms the quantitative profile results.

3.6.2 Typical worn surfaces for rubbers against PVC

Soft Rubber_PVC1_Slurry   Hard rubber_PVC1_slurry   Natural rubber_PVC1_Slurry

Sliding

Soft Rubber_PVC1_air   Hard rubber_PVC2_slurry   Natural rubber_PVC2_Slurry

Soft Rubber_PVC1_water   New rubber_PVC1_slurry
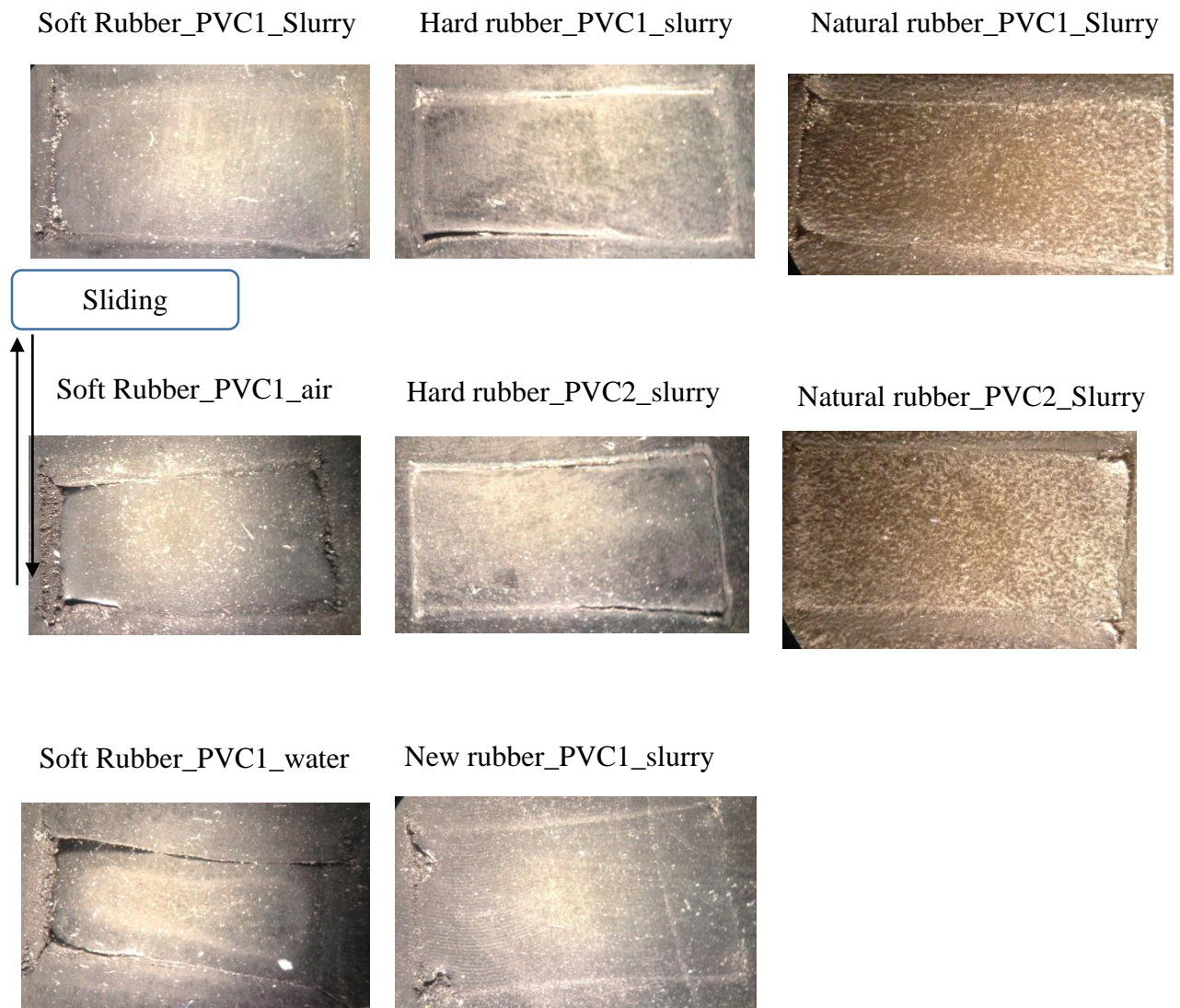
Figure 32. Worn surfaces of soft rubber, hard rubber, natural rubber and new rubber
against two different PVC material formulations

For the worn surfaces of rubber against PVC tests, as shown in Figure 32, visually the cracks on the edges seem less compared with the FRP tests, which also matches the profilometer wear measurements. This may be due to the FRP being a more abrasive material. New rubber and natural rubber have a better performance against wear than hard rubber and the soft rubber. There also appears to be cracking and possible cutting in some of the rubber tests due to edge effects. Note that cutting, cracking and tearing is all referring to the same observations, but the researchers are unsure of the specific mechanism actually causing the damage. The roughness of the natural rubber also visually appears to be different from the other types of rubber.

Chapter 4

Wear analysis of the PVC and FRP samples

4.1 Weight changes of the FRP and PVC samples

The weights of the PVC1, PVC2 and some FRP samples are measured before and after each slurry test. The change in weight is then calculated. The results are shown in Table 4 below. The data for the measurements are show in the tables below. However, as shown, the weight changes for both samples were smaller than the resolution of the scale and sometimes even positive, which suggests a gain in mass. This gain in mass could be due to some residual slurry material on the sample or the absorption of water. Overall the wear on these harder samples is negligible compared to the wear on the softer rubber. This is the expected result according to the accepted Archard theory of wear [24] which states that wear decreases with material hardness (i.e. softer materials usually wear faster than harder materials).

Table 4. Weight of the FRP and PVC samples

Slurry	PVC1 against New Rubber			PVC1 against Hard Rubber			PVC2 against Hard Rubber		
Unit: g	1	2	3	1	2	3	1	2	3
Before	0.38733	0.39381	0.37356	0.3739	0.36497	0.37819	0.3635	0.3922	0.3866
After	0.3873	0.39402	0.37354	0.37372	0.36488	0.3779	0.3635	0.3921	0.3866
Change	3E-05	-0.00021	2E-05	0.00018	9E-05	0.00029	0	1E-04	0

Slurry	PVC1 against Natural Rubber			PVC2 against Natural Rubber			FRP against Natural Rubber		
Unit: g	1	2	3	1	2	3	1	2	3
Before	0.3831	0.3844	0.4061	0.4166	0.412	0.3713	0.9755	0.8311	1.0471
After	0.383	0.3844	0.4061	0.4166	0.4119	0.3713	0.9765	0.8314	1.0484
Change	1E-04	0	0	0	1E-04	0	-0.001	-0.0003	-0.0013

4.2 Surface roughness changes of the FRP and PVC samples

In order to quantitatively observe the wear properties of the counter samples (FRP and PVC), we measured the surface roughness of the contact surfaces of these samples before and after each slurry test by using the profilometer. If the roughness of the contact surfaces changed, this indicates that the surface did wear when in contact with the sliding rubber samples. The roughness data are shown in Figures 33-36.

	Round 1	Round 2	Round 3
PVC1 Before	0.2275	0.2159	0.1735
PVC1 After	0.2671	0.2473	0.1809
PVC2 Before	0.5321	0.3608	0.2522
PVC2 After	0.5993	0.4712	0.2411
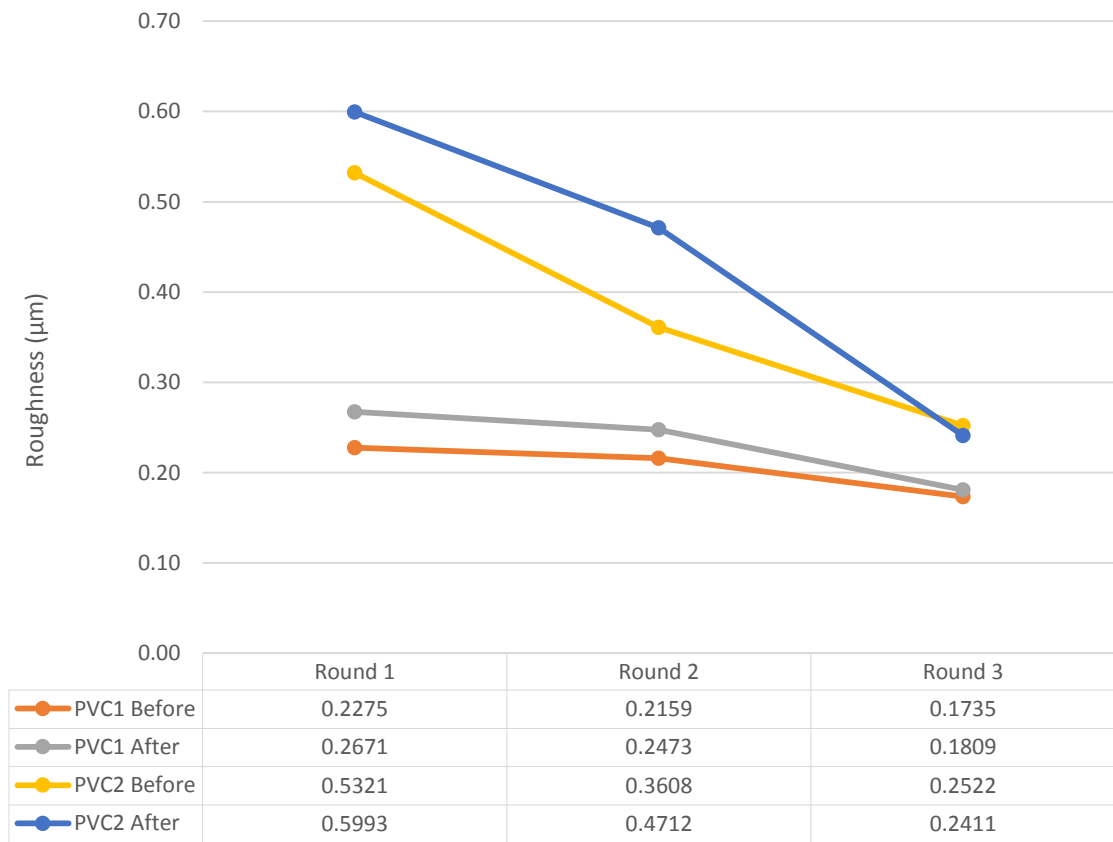
Figure 33. Surface roughness of PVC before and after the tests

	Round 1	Round 2	Round 3
Before	11.9622	13.3979	23.1742
After	13.8901	14.6773	27.5157

Figure 34. Surface roughness of FRP before and after the tests

The surface roughness of almost all of the samples were slightly increased after each test, especially for FRPs. Note that the counter samples and rubber samples were changed for every test. It shows that PVC and FRP did wear during the contact. The average change in roughness for PVC1 and PVC2 are calculated and shown in Fig. 35. It suggests that the PVC 1 might wear slightly differently than PVC2, but a more thorough analysis is needed to confirm this. The roughness changes of the FRP samples were calculated and compared with the values of the natural rubber wear of the sliding tests in order find if there is a relationship between the a change in roughness and wear measured via profilometry (see Fig. 36). There is also increased wear rate to higher roughness, which intuitively seems correct. This relationship appears to be confirmed.
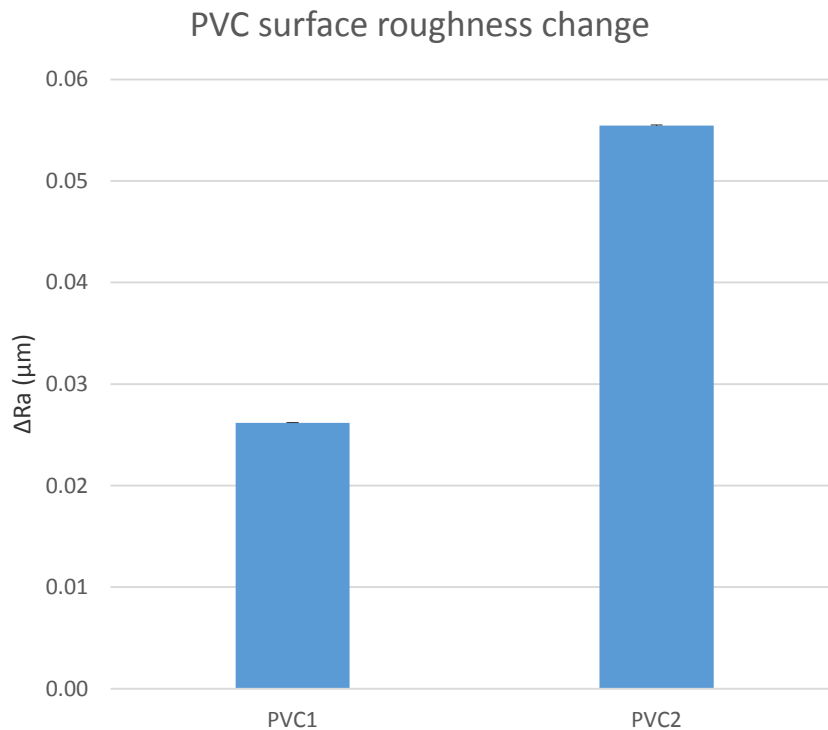
Figure 35. Average surface roughness change of PVC before and after the tests
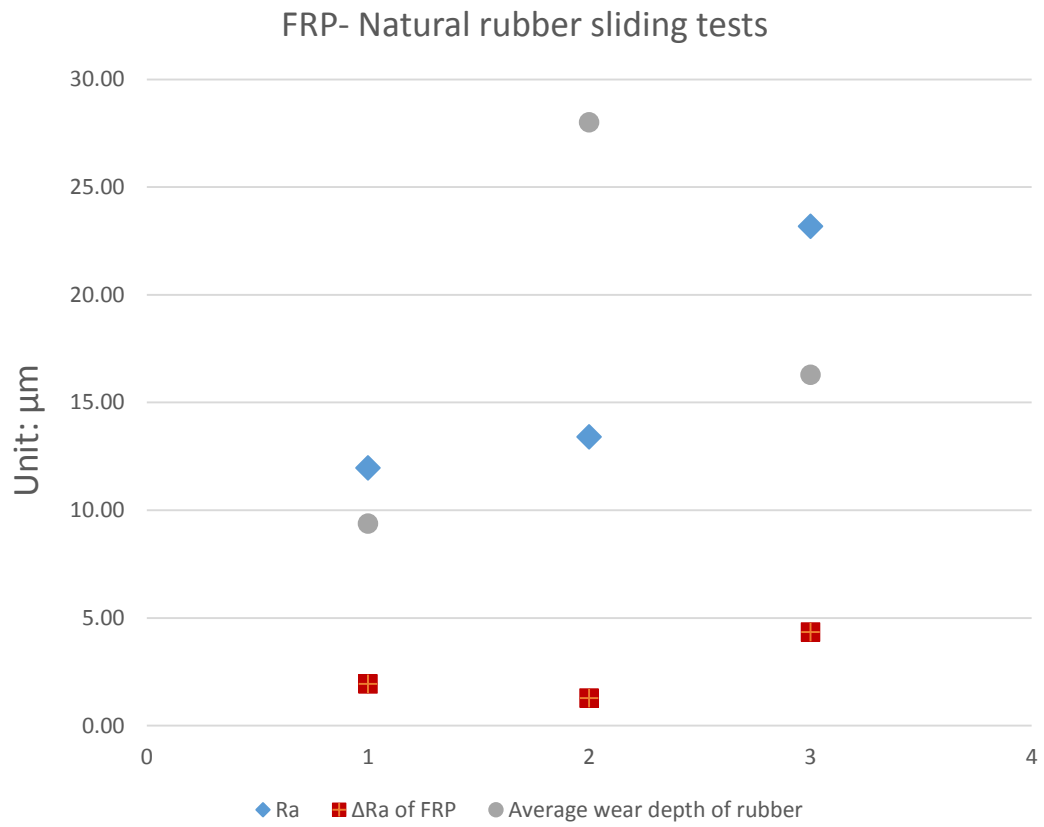
Figure 36. Surface roughness change of FRP before and after the tests

Chapter 5

Indentation test

5.1 Test set-up

In order to thoroughly characterize the mechanism of the rubber wear, an indention test without sliding was conducted to compare with the sliding tests. PVC1 samples were loaded normally against the new rubber material in air. Basically, without reciprocating motion of the lower rubber sample, a constant normal force of 100N was applied on the new rubber by the upper PVC1 sample for 3 hours, (i.e. the same time duration as the sliding tests).
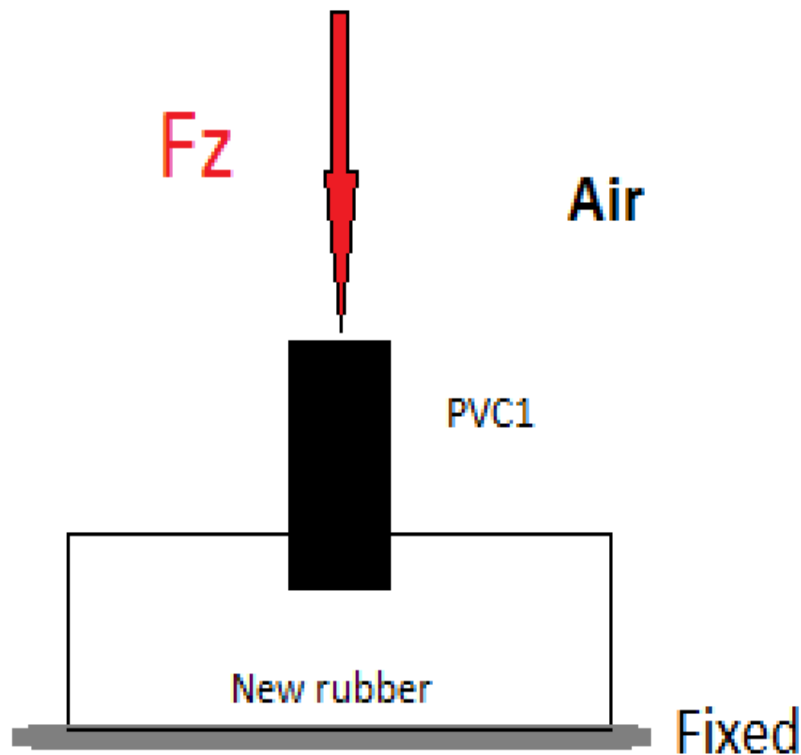
Figure 37. Schematic of the indention test

5.2 Results

The contour of the permanently deformed surface under compression were measured in both directions on the new rubber. Pictures of the loaded surface are also shown in Figure 38. No visible cracks or cutting appear to be present on the worn surface. Therefore, the cracking and cutting most only occur when sliding motion and a lateral force are present. This suggests that a portion of the damage to the rubber samples may be permanent set in the rubber that could cause the rubber part to loosen its contact with the FRP and PVC. This loosening could lead to more relative motion and sliding, which would also result in more wear.

Figure 38. Compressed surface
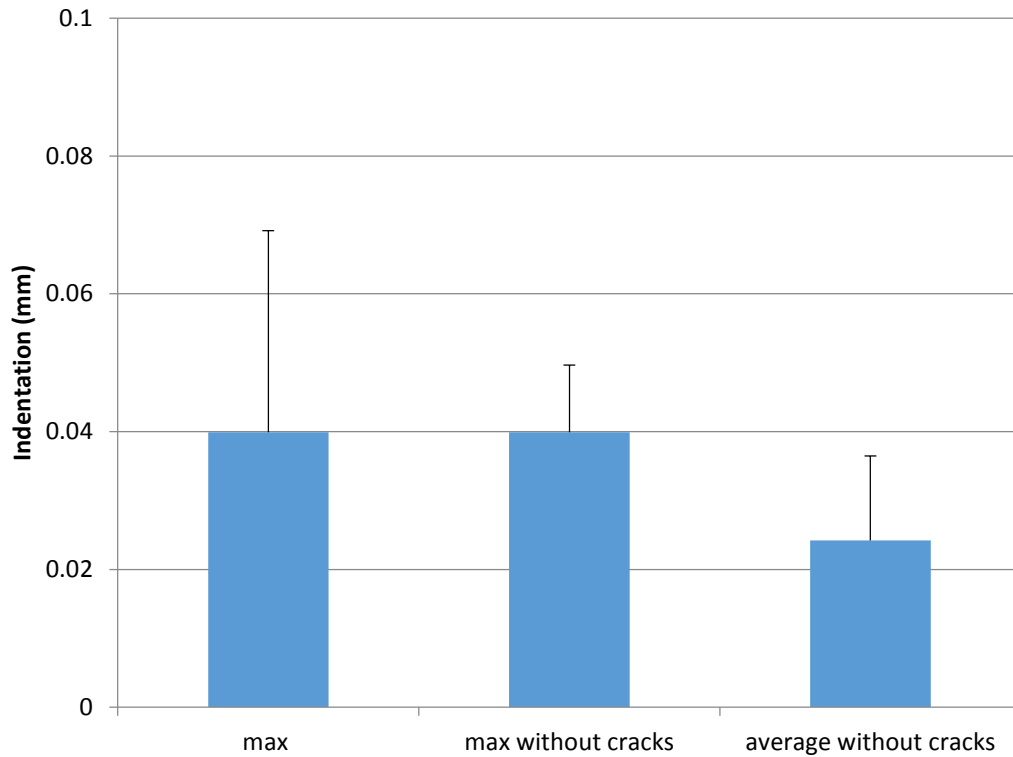
Figure 39. Wear depths of indentation test measured in both directions for new rubber in air

It is shown in Figure 39 above that the indentation depths of indentation test, compare the max value and the value of max without cracks, the difference is extremely small. As cracks are usually the reason for large wear depth, this also reveals that no significant cracks or cutting are formed in the stationary contact, while for the sliding motion case, cracks are shown on the edges of the contact region. The micro-vibration effect in stick-slip motion mentioned above could be a reason for the formation of the cracks.

Chapter 6

Experimental results of friction

6.1 Experimental results of friction force

The friction force is also recorded during the experiments. Because the motion of the upper rubber specimen is reciprocating, the trend of the friction force is periodic. The friction forces of the soft rubber against FRP in air, water, and slurry as a function of time are shown in Figure 40-43 respectively. All of them alternate between positive and negative values because the sliding direction of the rubber against FRP is changing with time. Thus, only the peak values of the positive part and the negative part are considered in order to make a comparison between the different lubricating conditions as well as different rubber in the same condition. The peak friction forces of the soft rubber and hard rubber against FRP are shown in Table 5 and 6.

Table 5. Peak Friction Force of Soft Rubber against FRP

Soft Rubber/ N	Positive Peak	Max	Min	Negative Peak	Max	Min
AIR	37.5	2.500E+00	-1.5	-37.0	2.000E+00	-3.0
WATER	35.7	1.833E+00	-3.2	-34.5	5.500E+00	-3.0
SLURRY	38.0	8.000E+00	-6.0	-37.2	5.667E+00	-7.8

Table 6. Peak Friction Force of Hard Rubber against FRP

Hard Rubber/ N	Positive Peak	Max	Min	Negative Peak	Max	Min
AIR	43.3	3.667E+00	-5.3	-43.3	7.333E+00	-5.2
WATER	46.3	1.667E+00	-1.3	-44.0	1.000E+00	-1.5
SLURRY	47.0	1.000E+00	-1.0	-47. 7	1.667E+00	-1.8
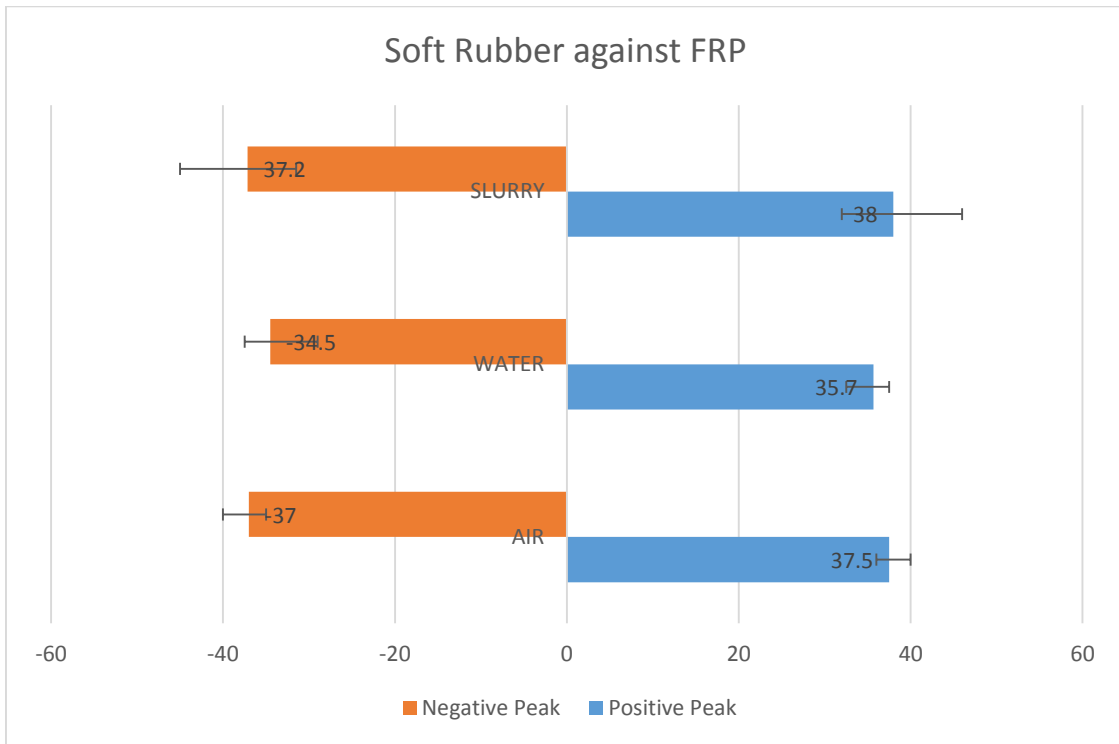
(a)
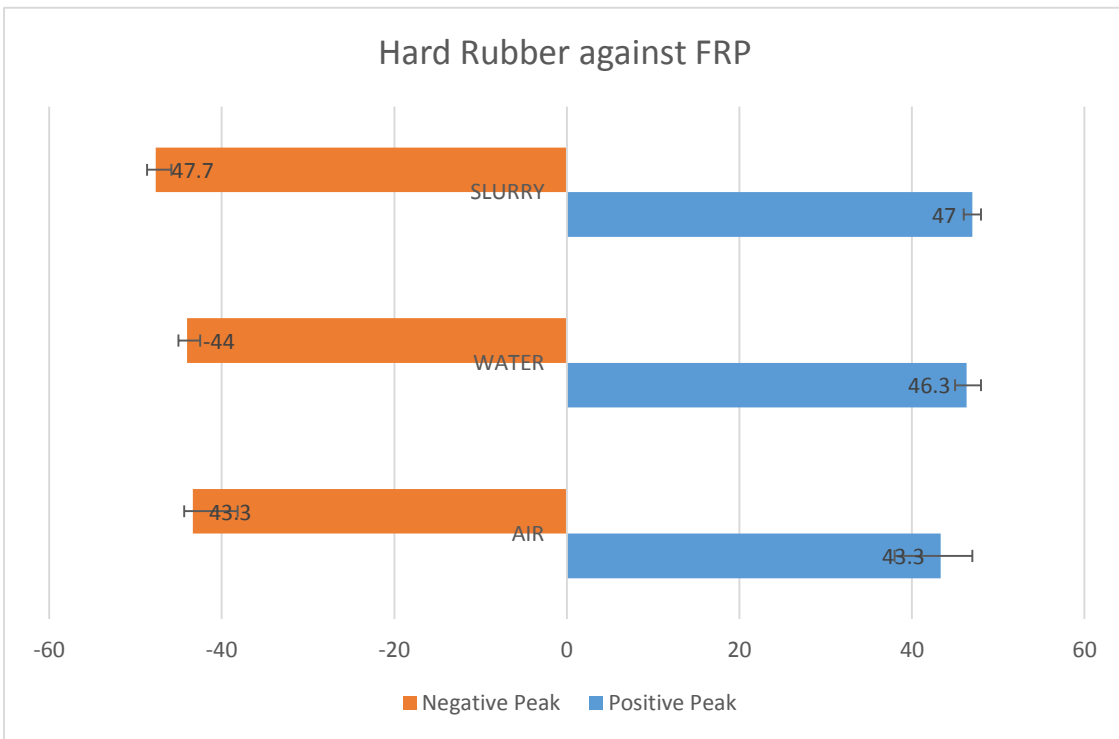
(b)

Figure 40 Peak friction forces of soft rubber and hard rubber against FRP

A clear comparison of the peak friction force in different cases with the error bar is shown in Figure 34. The error bars represent the difference between each peak value of the three tests for each case and the mean value. We can see that the peak values of hard rubber is significantly larger than the soft rubber for any of the lubricating conditions. But their values are more consistent because the error bars are relatively small. For the hard rubber against the FRP case, with lubrication, the peak friction forces are increased, especially for the slurry case. While for the soft rubber, the difference between air, water and slurry cases are not significant and the smallest peak friction forces of both positive and negative is the water case. And the values are really close to each other for the slurry case and the air case, but the error bar is larger for the slurry case. The reason for these results probably is that the soft rubber is more elastic and because of the relatively small sliding distance and large reciprocating frequency, the deformable part of the soft rubber in the contact region has a big influence on the friction.
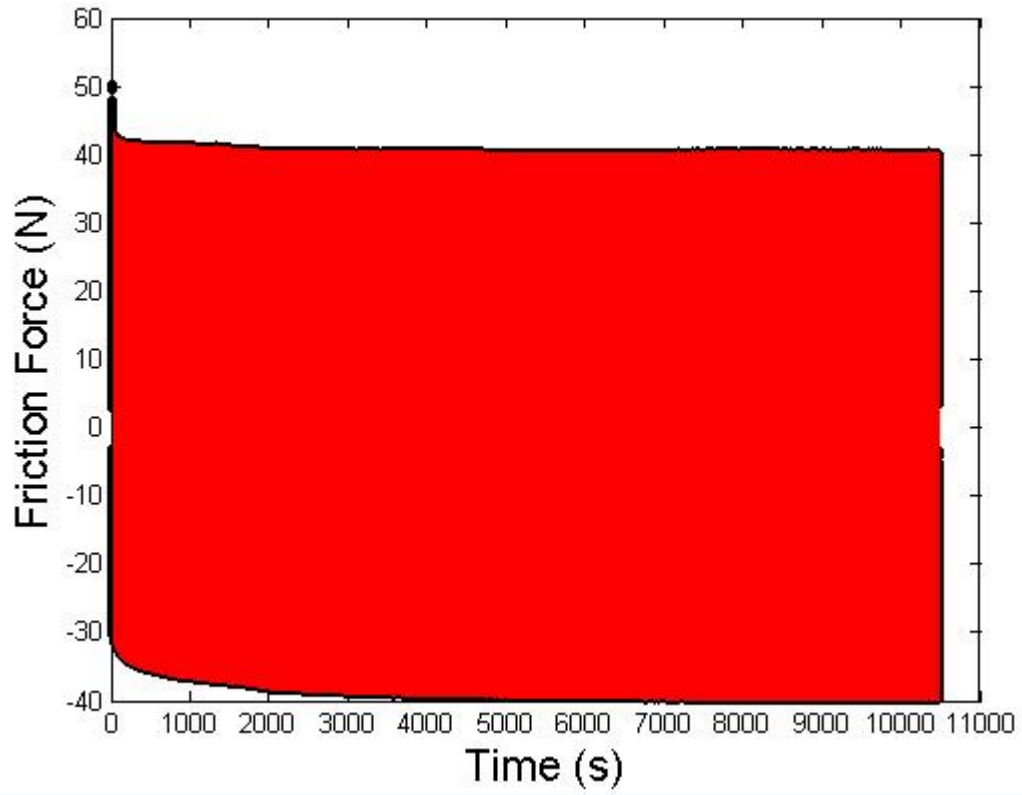
(a)
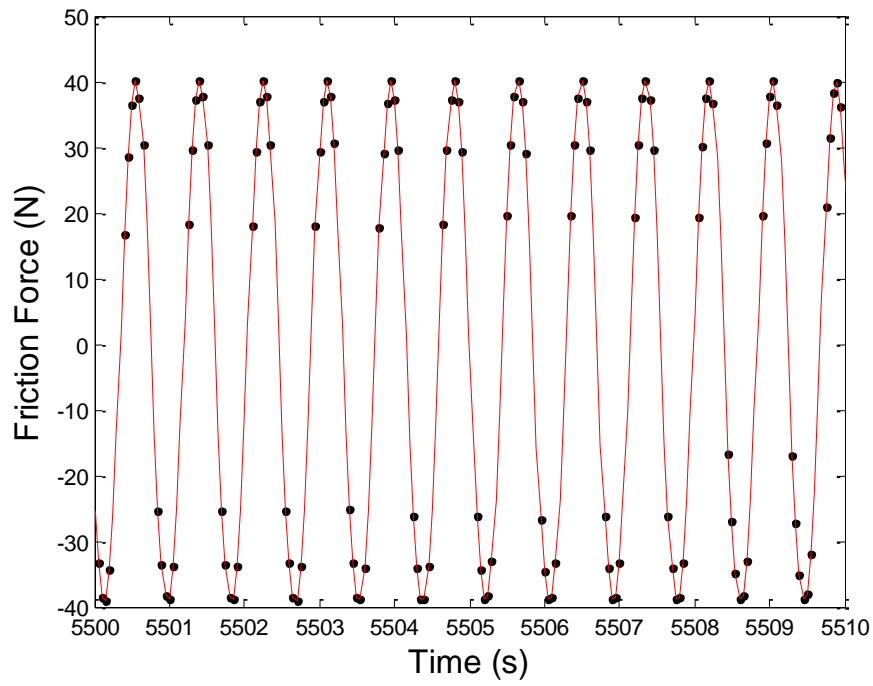
(b)

Figure 41. Friction force over time of soft rubber against FRP in air
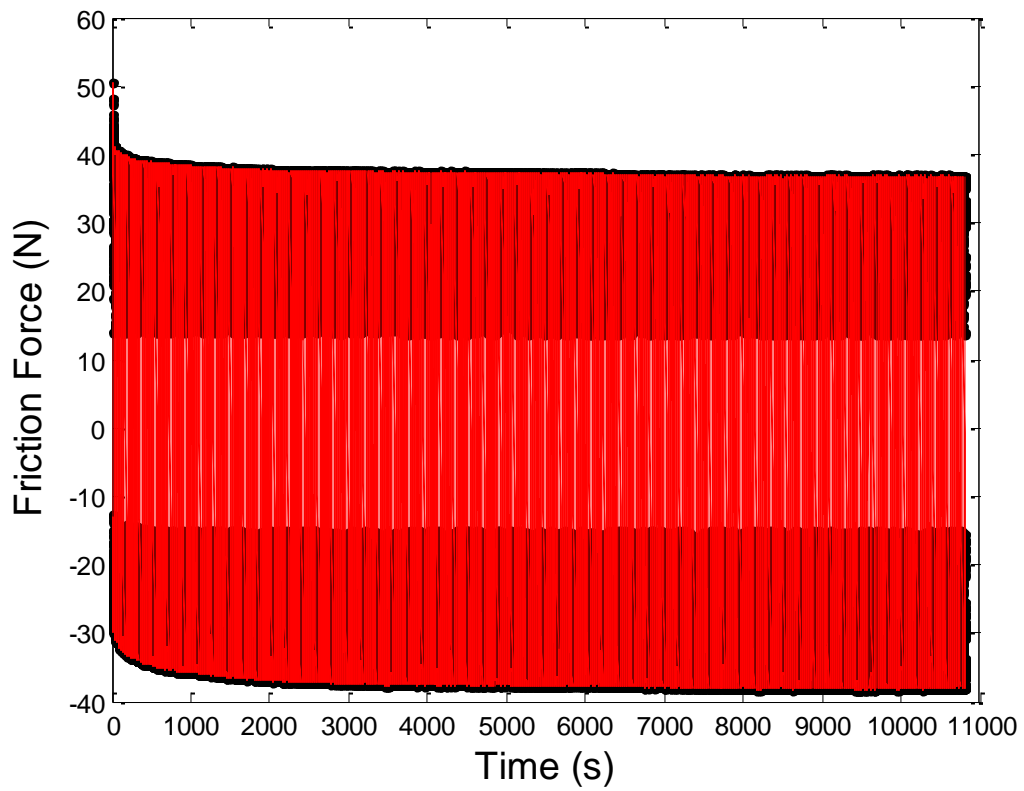
(a)
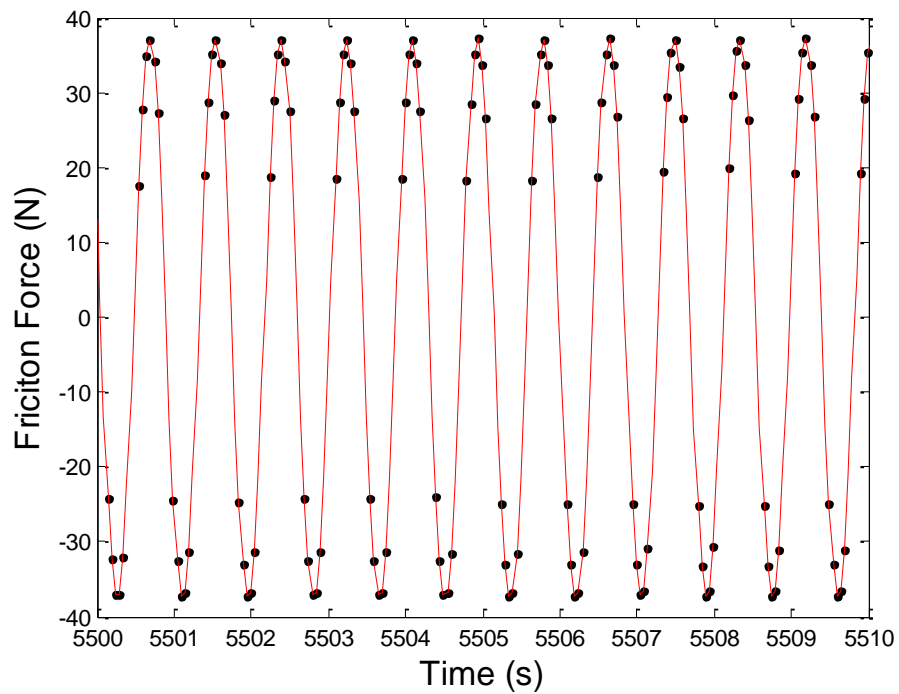
(b)

Figure 42. Friction force over time of soft rubber against FRP in water
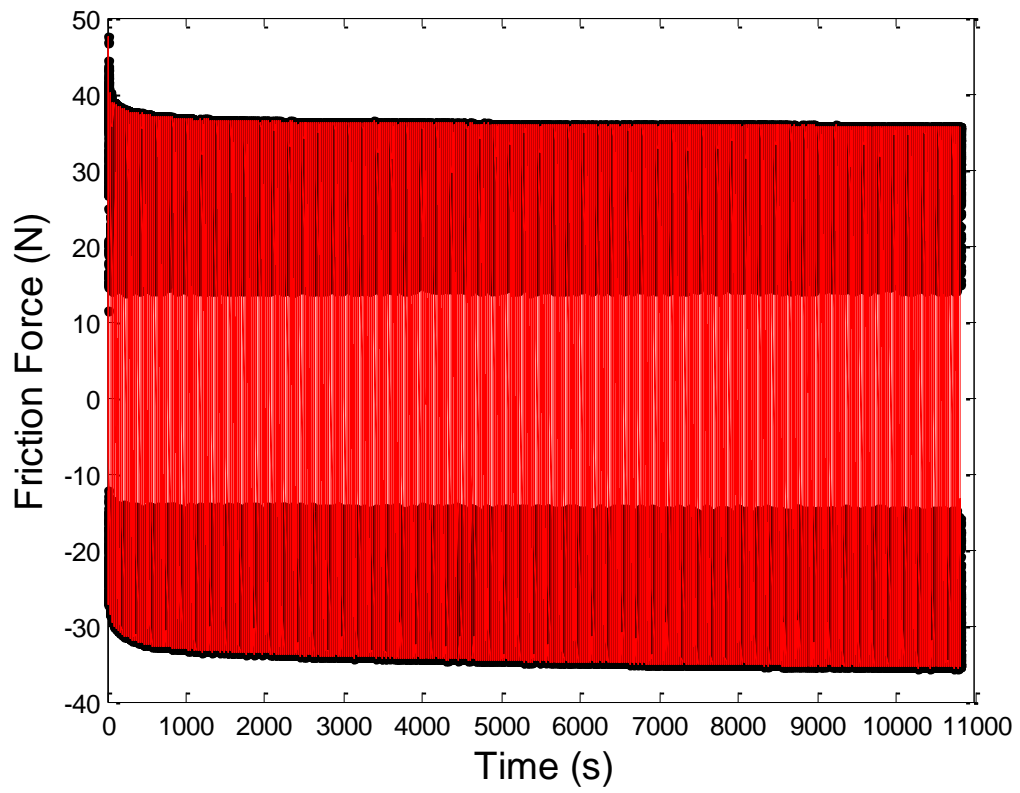
(a)
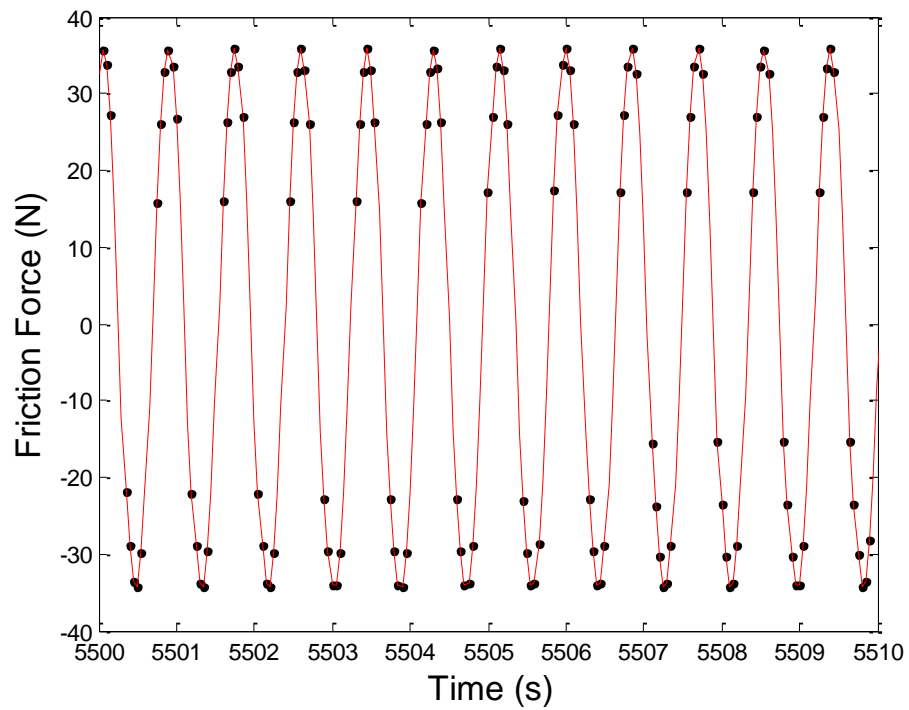
(b)

Figure 43. Friction force over time of soft rubber against FRP in slurry

Figure 41 to figure 43 show the variation of friction force as a function of time during the reciprocating motion. Bhattacharya et al [25] thought that the initial micro-cracks and the later propagation was caused by the 'periodic bumping'. As the time range increased, more reciprocating cycles are applied to the rubber. Because of the block of the deformation part in front of and behind the upper samples, the upper specimen just sticks into the rubber samples and keep still with no sliding relate to the rubber samples. The ripples were formed during the sliding process and because of the reciprocating motion, the rubber surface is straining alternatively. In this way, due to the fatigue mechanism, the tip of the ripples are easily torn apart to form the debris, which are generally the main contributor to rubber wear. Relative sliding motion is gradually dominated as more permanent deformation on the contact area of rubber samples are formed. At first, deformation dominates while after the formation of the permanent deformation, the relative reciprocated sliding between the rubber and the harder materials may cause fretting on the rubber surface.

6.2 Coefficient of friction of rubber against FPR

During the entire duration of each test, the friction force and the normal load are recorded according as a function of the time. The coefficient of friction is also calculated by dividing the friction force by the normal load. Because the motion of the upper rubber specimen is reciprocating, the trend of the friction force is periodic. In this way, the COF calculated at every point in time are also distributed in a range. The coefficients of friction of soft rubber against FRP in air, water and slurry changing with the time are shown respectively in Figure 44-47. Because the COF is a scalar, its magnitude is not related to the direction of the friction force. In this part, the median COF were found for each case in order to make a comparison, the results are shown in the Figure 44.

	AIR	WATER	SLURRY
SOFT RUBBER	0.301866667	0.290533333	0.2431
HARD RUBBER	0.354133333	0.3567	0.3756
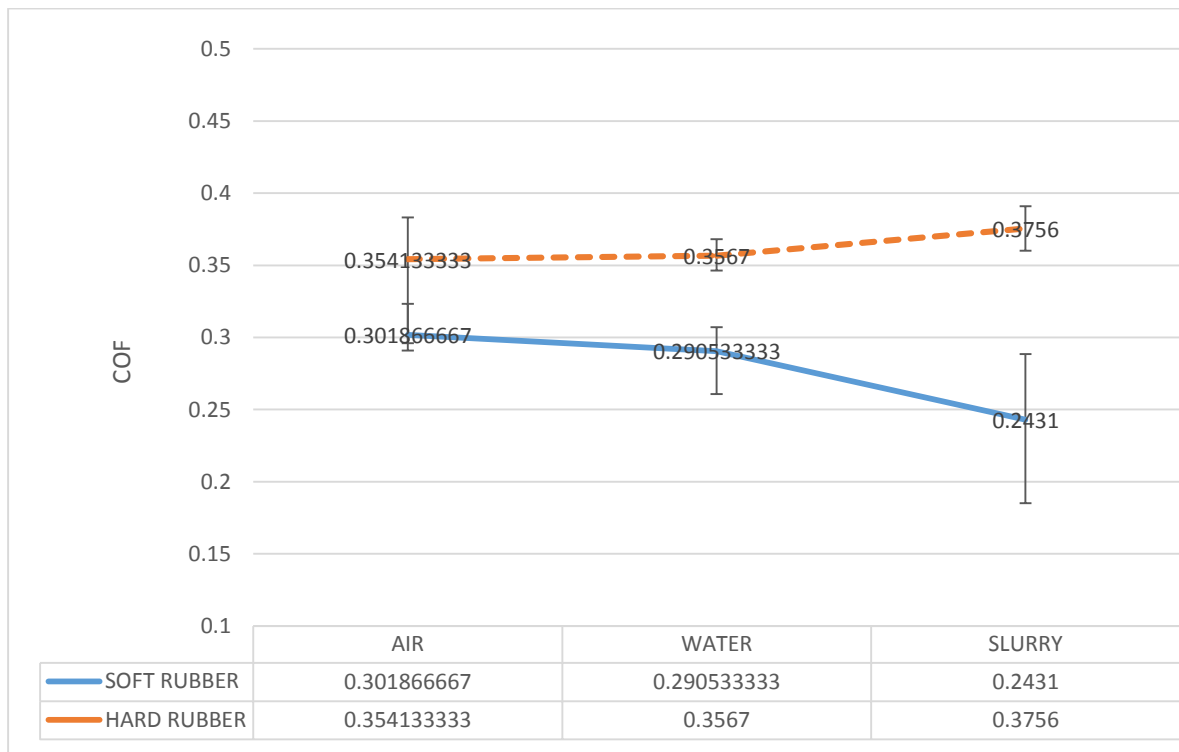
Figure 44. COF of soft rubber and hard rubber against FRP
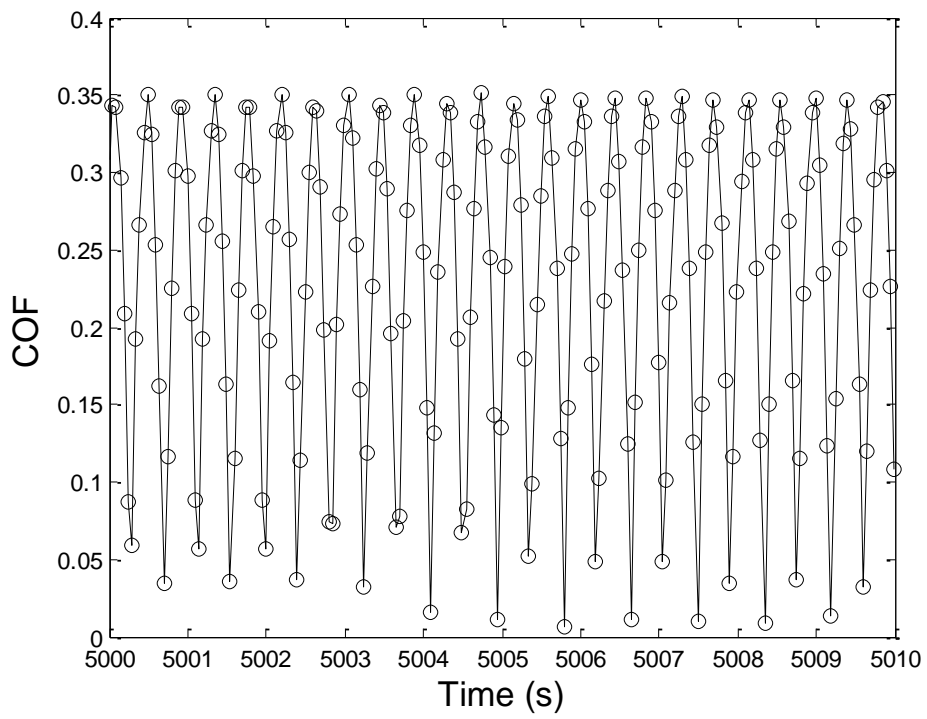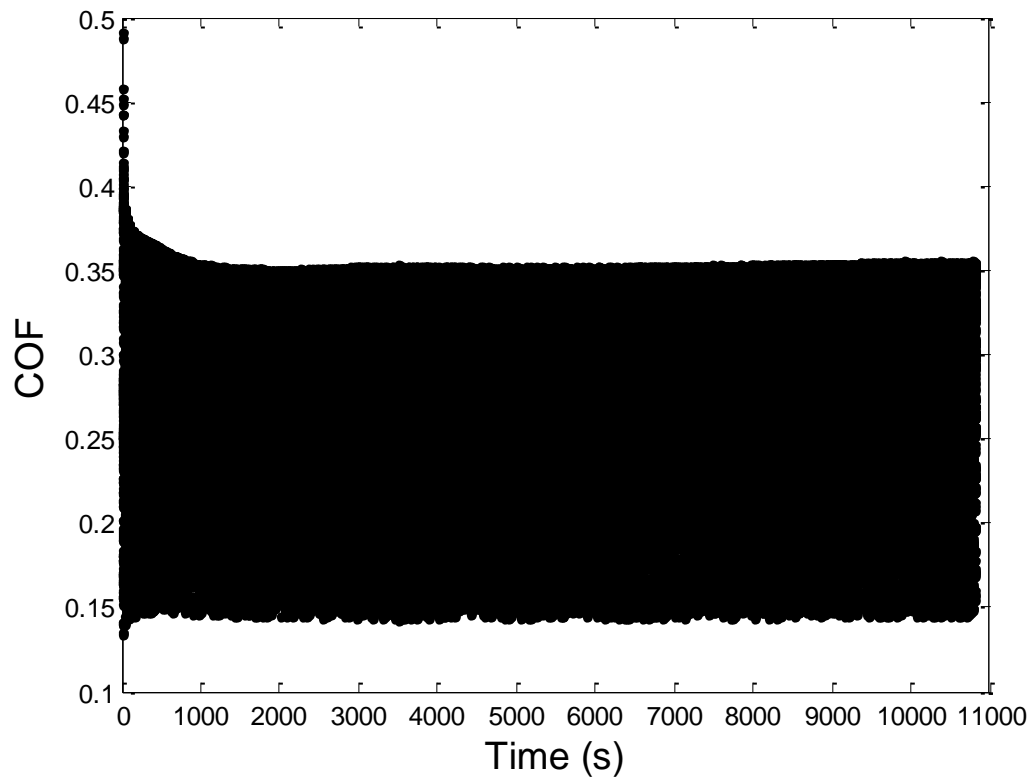
Figure 45. COF of soft rubber against FRP in air
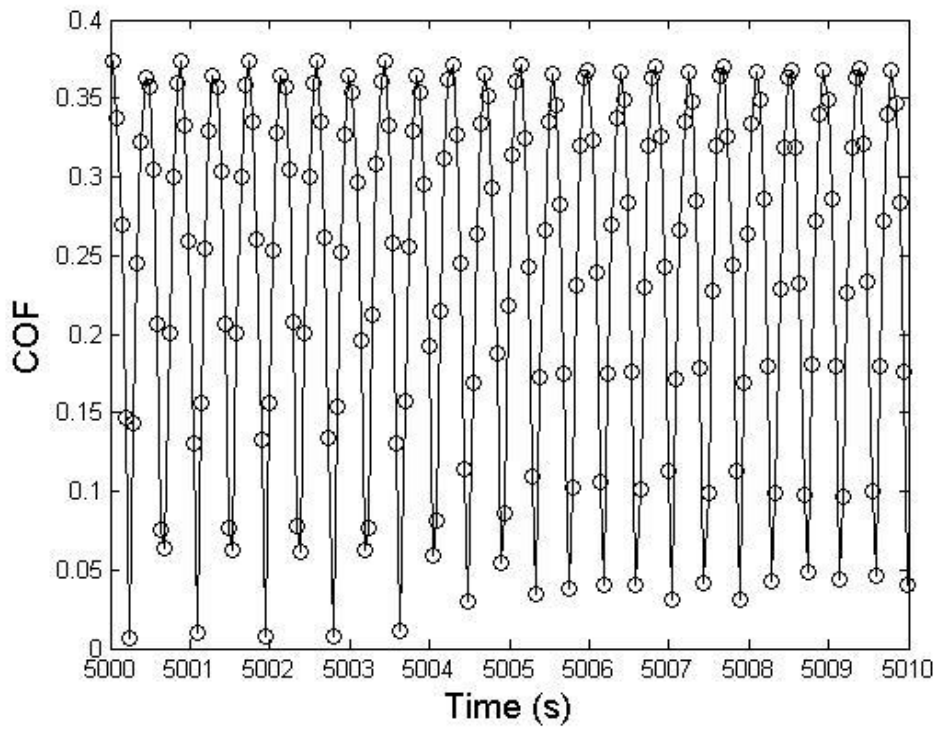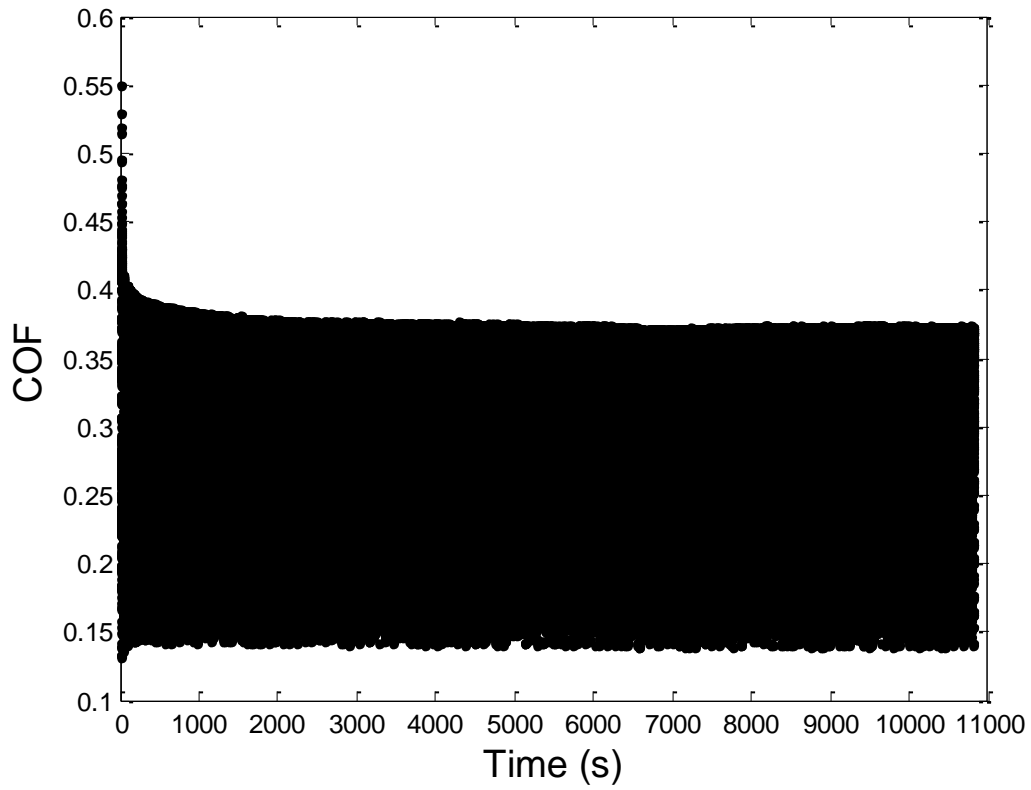
Figure 46. COF of soft rubber against FRP in water
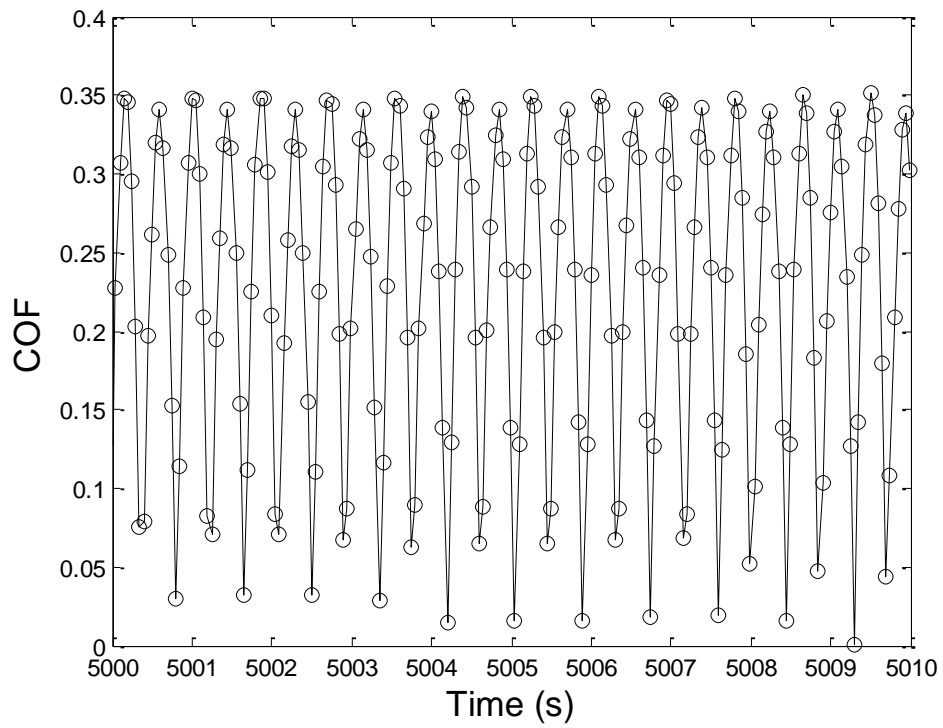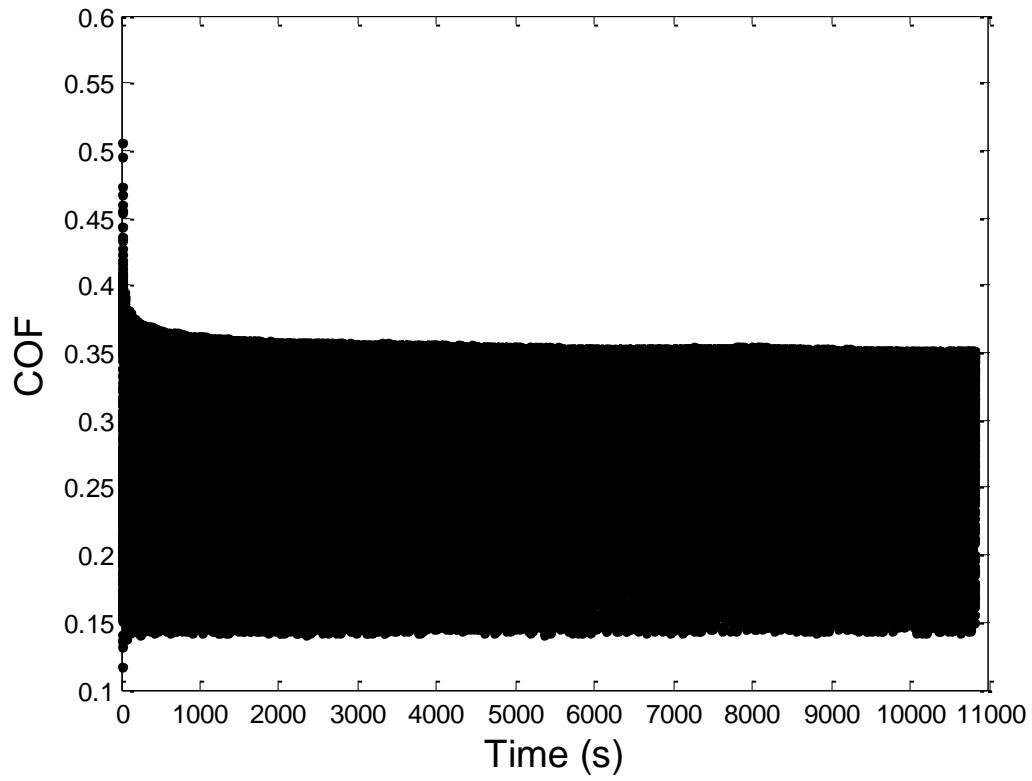
Figure 47. COF distribution of soft rubber against FRP in slurry

Chapter 7

Conclusions and recommendations

7.1 Conclusions

1) Six rounds of tests for the following material pairs have been completed,

   FRP on Hard Rubber, Soft Rubber, New Rubber and Natural Rubber,

   PVC1 on New Rubber, Soft Rubber, Hard Rubber and Natural Rubber,

   PVC2 on Hard Rubber and Natural Rubber.

2) For hard rubber in air, water and slurry, cracks are negligible compared with the wear on the worn surfaces. And it has less wear against FRP than the PVC. Compared with PVC1, hard rubber against PVC2 had smaller wear depth in air, water and slurry. In addition, the water and slurry decreased the wear and cracking during the sliding tests.

3) Soft rubber displayed more cracking than the other rubbers. It also had more wear against FRP than PVC. In addition, the water and slurry did increase the wear of soft rubber in the sliding tests.

4) Natural rubber had the least wear when sliding against PVC in slurry. It had more wear in the sliding tests against FRP than PVC.

5) New rubber had the smallest wear depth in both directions against FRP. It shows the best anti-wear performance overall. The slurry has a positive effect on decreasing the wear for new rubber in the sliding tests. In addition, some cracks also can be found in the wear region.

6) From the indentation test, no cracks are shown for the new rubber against PVC. Therefore, sliding is probably the main reason for cracks, but loading and stress concentrations at the edge of contact could also contribute. In addition, the new rubber did compress and the depth values are similar to the wear depth values of the new rubber against PVC1 tests.

7) The edges of the samples could also be helping to cause high stresses and thus cracking, tearing or cutting.

7.2 Future recommendations

1) Perform long term tests to measure the wear on the PVC and FRP quantitatively.

2) The effect of frictional heating and temperature should be considered during the rubber wear contact experiments. This could be done by monitoring the temperature change of the contact region.

3) Reduce the load on the tests to reduce the occurrence of cracking, while still inducing wear.

4) Locate and evaluate alternative materials for the FRP to PVC interface. Rubber is a very non-wear resistant material and is the weak link. Other materials might provide an interface with a longer life. Wear resistant coatings, greases, or finishes might also be an option.

5) Apply the finite element method to make a three dimensional model and to incorporate the actual properties of the different types of rubber for the simulation. This can be used to confirm the source of cracking and the relatively pressure distribution. This might also be adapted to actually design geometries that reduce the stress and wear.

References

[1] P.Nam, S. (1986). Tribophysics. Englewood Cliffs: Prentice-Hall.

[2] Jain V K, B. S. (1978). Material transfer in polymer-polymer sliding. Wear, 46(1): 177-188.

[3] Birkett A, L. J. (1986). Counterface effects on the wear of a composite dry-bearing liner. Wear, 110(3): 345-357.

[4] Barrett T S, S. G. (1992). Effect of roughness and sliding speed on the wear and friction of ultra-high molecular weight polyethylene. Wear, 153(2): 331-350.

[5] F, P. D. (1984). Counterface roughness effect on the dry steady state wear of self-lubricating polyimide composites. Journal of tribology, 106(2): 177-184.

[6] Deli G, Q. X. (1991). Physical models of adhesive wear of polytetrafluoroethylene and its composites. Wear, 147(1): 9-24.

[7] Stachowiak G, B. A. (2013). Engineering tribology. Butterworth-Heinemann.

[8] Atkinson J R, B. K. (1978). The wear of high molecular weight polyethylene—Part I: the wear of isotropic polyethylene against dry stainless steel in unidirectional motion. Journal of Tribology, 100(2): 208-218.

[9] Schweitz J Å, Å. L. (1986). Mild wear of rubber-based compounds. Friction and Wear of Polymer Composites, 289-327.

[10] A, S. (1971). How does rubber slide? Wear, 17(4): 301-312.

[11] Persson B N J, T. E. (2000). Qualitative theory of rubber friction and wear. The Journal of Chemical Physics, 112(4), 112(4): 2021-2029.

[12] Persson, B. (1988). Model study of brittle fracture of polymers. Physical review letters, 81(16): 3439.

[13] Persson, B. N. (2009). Theory of powdery rubber wear. Journal of Physics: Condensed Matter, 21(48): 485001.

[14] Persson, B. N. (2014). Role of Frictional Heating in Rubber Friction. Tribology Letters, 56(1): 77-92.

[15] Persson, B. N., Volokitin, A. I., & Ueba, H. (2011). Phononic heat transfer across an interface: thermal boundary resistance. Journal of Physics: Condensed Matter, 23(4): 045009.

[16] Persson, B. N. (2014). Thermal interface resistance: cross-over from nanoscale to macroscale. Journal of Physics: Condensed Matter, 26(1): 015009.

[17] Fukahori, Y., Liang, H., & Busfield, J. J. (2008). Criteria for crack initiation during rubber abrasion. Wear, 265(3): 387-395.

[18] Fukahori, Y., & Yamazaki, H. (1994). Mechanism of rubber abrasion. Part I: Abrasion pattern formation in natural rubber vulcanizate. Wear, 171(1): 195-202.

[19] Veeco. (n.d.). Dektak 150 Profiler User's manual.

[20] Gibson, R. F. (2011). Principles of Composite Material Mechanics, Third Edition. CRC Press.

[21] Hassan M M, El-Megeed A, Maziad N A. (2009). Evaluation of curing and physical properties of NR/SBR blends using radiation-grafting copolymer [J]. Polymer Composites, 30(6): 743-750.

[22] Butyl Rubber Sheets. (2015). Retrieved from ZENITH Industrial Rubber Products PVT. LTD. Web Site: http://www.zenithrubber.com/rubber-sheets/butyl-rubber-sheets.htm.

[23] Fischer, I. S.-C. (2014). Ullmann's Encyclopedia of Industrial Chemistry. 1–30.

[24] Archard J F. (1953). Contact and rubbing of flat surfaces [J]. Journal of applied physics, 24(8): 981-988.

[25] Bhattacharya, M., & Bhowmick, A. K. (2010). Analysis of wear characteristics of natural rubber nanocomposites. Wear, 269(1), 152-166.

Appendix 1

Schematics of Test Rig Parts

Appendix 2